Aus der

Universitätsklinik für Radioonkologie mit Poliklinik

Endothelial-cell-induced radioresistance in glioblastoma

Inaugural-Dissertation

zur Erlangung des Doktorgrades

der Medizin

der Medizinischen Fakultät

der Eberhard Karls Universität

zu Tübingen

vorgelegt von

Haehl, Erik

2021

Dekan:	Professor Dr. B. Pichler
1. Berichterstatter:	Professor Dr. D. Zips
2. Berichterstatter:	Professorin Dr. B. Schittek
Tag der Disputation:	21.12.2020

für Sibylle Haehl

Table of contents

1 Introduction 10

1.1 Glioblastoma 10

1.2 Cancer stem cell (hypothesis) 11

1.3 Glioblastoma stem-cell-like cells 12

1.4 Glioblastoma stem cell niche 12

1.5 Research questions/Aim of this work 13

2 Material and methods 14

2.1 Routine cell culture procedure 14

2.2 Endothelial cell lines 14

2.2.1 Human umbilical vein endothelial cells (HUVEC) 14

2.2.2 Human cerebral microvascular cells (hCMEC/D3) 15

2.3 Glioblastoma cell lines 16

2.3.1 T98G 16

2.3.2 U87MG Katushka 17

2.4 Endothelial-Glioblastoma Co-culture 18

2.4.1 Direct contact co-culture 19

2.4.2 Indirect co-culture 19

2.4.3 Transfilter co-culture 20

2.5 Irradiation 21

2.6 SDF-1 Immunofluorescence microscopy 21

2.6.1 Concept 21

2.6.2 Procedure (modified from Edalat, Stegen, Klumpp, Haehl et al., [55]) 21

2.7 Colony formation assay 22
2.7.1 Concept 22
2.7.2 Procedure 22
2.7.3 Treatment 23
2.8 Flow cytometry 24
2.8.1 Concept 24
2.8.2 Procedure 24
2.8.3 Treatment 25
2.9 Quantitative RT-PCR 25
2.9.1 Concept 25
2.9.2 Procedure and primers 25
2.9.3 Treatment 28
2.10 Patch-clamp recording 28
2.10.1 Concept 28
2.10.2 Procedure (modified from Edalat, Stegen, Klumpp, Haehl et al., [55]) 29
2.11 Migration assay 30
2.11.1 Concept 30
2.11.2 Procedure 30
2.11.3 Treatment 31
3 Results 32
3.1 Co-culture with HUVEC (Human umbilical vein endothelial cells) 32
3.1.1 SDF-1 Immunofluorescence 32
3.1.2 Flow cytometry 34
3.1.3 Colony formating assay 35

3.2 Co-culture with hCMEC/D3 (human cerebral microvascular endothelial cells) 36
3.2.1 Flow cytometry 36
3.2.2 Colony formating assay 37
3.2.3 Reveres Transcription Polymerase Chain Reaction 38
3.2.4 Patch-clamp recording 41
3.2.5 Migration assay 45
4 Discussion 46
4.1 Summary of results 46
4.2 Addressing the research questions 47
4.3 Co-culture model 53
4.4 Conclusion and further perspective 55
5 Summary 56
6 Zusammenfassung 58
7 Literature 60
8 Erklärung zum Eigenanteil 65
9 Veröffentlichungen 66
10 Table of figures 67
11 Danksagung 71
12 Appendix 72

Abbreviations

ACTB	=	Beta-Actin
ATCC	=	American Type Culture Collection
BK	=	BK Potassium Channel
BSA	=	Bovine Serum Albumin
Ca	=	Calcium
CDS	=	Cell Dissociation Solution
CFA	=	Colony Formation Assay
Cl	=	Chloride
CSC	=	Cancer Stem Cell
CXCR4	=	CXC-Motiv-Chemokinrezeptor 4
DAPI	=	diamidino-2-phenylindole
DNA	=	Deoxyribonucleic Acid
DSMO	=	Dimethyl Sulfoxide
EC	=	Endothelial Cell
EGF	=	Epidermal Growth Factor
FCS	=	Fetal Calv Serum
FGF	=	Fibroblast Growth Factor
GAPDH	=	Glyceraldehyde 3-Phosphate Dehydrogenase
GB	=	Glioblastoma
GCS	=	Glioblastoma Stem Cell
Gy	=	Grey
hCMEC	=	Human Microvascular Endothelial Cell
HUVEC	=	Human umbilical vein endothelial cell
IDH	=	Isocitrate Dehydrogenase
IgG	=	Immunglobulin G
IK	=	IK Potassium Channel
K+	=	Potassium
Kat	=	Katuschka-Protein
LINAC	=	Linear Particle Accelerator
Mg	=	Magnesium
MGMT	=	O6-Methylguanin-DNA-Methyltransferase

MMP	=	Matrix Metallopeptidases
mRNA	=	Messenger Ribonucleic Acid
n	=	Number
Na	=	Sodium
Oct4	=	Octamer-Binding Transcription Factor 4
p	=	probability value
PBS	=	Phosphate-Buffered Saline
PDHB	=	Pyruvate Dehydrogenase Beta
rh	=	Recombinant Human
RPMI	=	Roswell Park Memorial Institute
RT-PCR	=	Reverse Transcription Polymerase Chain Reaction
SDF-1	=	Stromal Cell-Derived Factor 1
SE	=	Standard Error
TGF-beta	=	Transforming growth factor Beta
TGF-b-R	=	Transforming growth factor Beta Receptor
TRPM8	=	Transient Receptor Potential Melastin 8
vWF	=	von Willebrand Factor

1 Introduction

1.1 Glioblastoma

Glioblastoma is the most frequent malignant primary brain tumour in adults with 0.59 – 3.69 new diagnoses per 100,000 persons and year, a median age of 64 years and a notably higher incidence rate in men with 3.97 vs. 2.53 in the US [1, 2]. It's classified as a grade IV brain tumour by the world health organisation which is the category for the most aggressive and rapidly growing brain tumours. The macroscopic tumour is typically located in the cerebral hemispheres, seldomly crossing the corpus callosum, and characterized by extensive vascularization, necrotic areas on the inside and an early invasive growth to macroscopic unaffected areas[3-5]. Despite the name glioblastoma, the cellular origin of these tumours remains subject of discussion with growing evidence that not glial cells but proneural stemcells form the predecessor of this malignancy [6-8]. Glioblastoma are categorized by their exhibition of the Isocitrate dehydrogenase (IDH), an enzyme crucial for any cells' aerobe metabolism, into IDH wildtype and IDH mutant glioblastoma[9]. The first also described as primary or de novo glioblastomas make up for around 90% of patients, usually with an older age of affection and a short clinical history. Whereas the rarer IDH mutant or secondary glioblastomas develop from a precursor lesion such as low-grade astrocytic gliomas in younger patients [9]. The standard treatment of the glioblastoma consists of radical/extensive surgical resection of the macroscopic tumour followed by radiotherapy combined with concomitant and adjuvant maintenance chemotherapy with the alkylating agents temozolomide or lomustine [10-12]. Even after trimodal therapy, prognosis remains poor to this date with a total 5-year survival of 9.8% and a median survival of 14.6 months [11]. The strongest prognostic factor is the epigenetic methylation status of the MGMT gene[11, 13], a DNA repair protein, with a median survival of 12.6 months in the unmethylated MGMT fraction versus 23.4 months in the methylated MGMT fraction that also benefits most from temozolomide [11]. Other prognostic factors include the extent of surgical resection and the age at

diagnosis. Nevertheless, even in most advantageous conditions true long-term survival or cure is not possible in most cases and nearly all patients face tumour recurrence within a few months [11, 13, 14].

Further analysis of the recurrence pattern of glioblastoma patients who underwent the described standard treatment shows that 79% of the patients experience local tumour recurrence defined as within the surrounding 2 cm of the resection cavity. Another 10% experiencing both local and distant tumour recurrence [15]. Furthermore, 72-77% of the glioblastoma recurrences occur within the 95% isodose line of the preceding radiotherapy receiving at least 57 Gy [14, 16, 17]. Taken together standard treatment has proven to considerably prolong progression-free and overall survival[11, 12], but in most cases in-loco recurrence is inevitable.

1.2 Cancer stem cell (hypothesis)

The cancer stem cell hypothesis based on the observation of tumour heterogeneity. Resembling the hierarchy in normal proliferating tissue it postulates a hierarchy of cells inside malignancies with a broad mass of differentiated tumour cells and a subpopulation of cancer stem cells. Those are characterized by self-renewal, radioresistance, chemoresistance and, most importantly, the potential of tumour initiation [18]. Initially, the cancer stem cell hypothesis was developed for certain leucaemias[19-21] and has then been extended and established for a variety of solid tumours, including breast cancer[22], colon cancer[23] and lung cancer[24, 25]. The assumption of a small therapy resistant subpopulation with the capability of tumour initiation could be one explanation for in-loco recurrences and late metastatic spread after macroscopic tumour remission. In order to cure these neoplastic diseases, therapy has not only to focus on the gross majority of differentiated tumour cells but on this specific subpopulation of stem cells [26, 27].

1.3 Glioblastoma stem-cell-like cells

With the in-loco recurrence as the predominant recurrence pattern in glioblastoma, the cancer stem cell hypothesis would be a possible explanation for the therapy failure described in 1.1. First *in vitro* data reporting a subpopulation of tumour initiating cells regarding brain tumours were published by Ignatova et al. by describing morphologically stem-like cells inside glial brain tumours that could differentiate into neural and astrocytic lineages [28]. Shortly after, Singh et al. identified a CD133-positive subpopulation featuring extended capabilities of self-renewal and tumour initiation in xenograft models [29], in contrast to CD133-negative cells. In the following research efforts, the description of glioblastoma stem-cell-like cells (GSC) has been specified as subpopulation with the ability of self-renewal, the capability of differentiation [30], a high DNA repair capacity [31], chemoresistance [32, 33], radioresistance [34-39] and tumour formation through implantation [40]. Several markers of stem-cell-like glioblastoma cells have been brought into discussion such as the cell surface marker CD133 (Prominin)[41], the cytoskeletal protein Nestin[40], the RNA binding protein Musashi and the transmembrane protein Notch[36, 42, 43].

1.4 Glioblastoma stem cell niche

When the cellular level of observation is widened to a more comprehensive approach concerning the tumours microenvironment it can be shown that like neuronal stem cells [44] the glioblastoma stem-cells-like cells aren’t randomly spread across the tumour bulk but can preferably be found in perivascular niches[45-47]. Namely CD 133 and Nestin positive cells, identified as glioblastoma stem-cell-like cells, were found in close proximity to intratumoral vessels [45, 48]. Interestingly, the niches vessels are often of immature and instable morphology and therefore only provide insufficient nutrition and oxygen supply [49, 50]. Apart from nurture, these niches seem to be crucial for the induction of the GSCs properties and an important factor in their maintenance [45]. Co-culturing glioblastoma with endothelial cells even enriches the CD133+ cell fraction and increases the expression of CD133 and other genes associated

with stem cell properties in glioblastoma cells [48, 51]. Concomitantly the presence of these endothelial cells promotes the ability of tumoursphere formation *in vitro* and *in vivo*, as a marker of self-renewal[48]. *In vivo*, previous co-culturing with endothelial cells accelerates the general tumour growth in an intracranial mouse xenograft model [52].

1.5 Research questions/Aim of this work

The proximity of glioblastoma stem-cell-like cells to tumour vessels could be a mere epiphenomenon of other processes. The reported findings point otherwise and suggest at least the induction of a stem-cell-like morphology in glioblastoma cells through endothelial interaction. It is unknown, if the enrichment of CD-133 or sphere formation translates onto a functional level and enables the hypothesized stem cell features in those cells. This would be of high interest to further support the cancer stem cell hypothesis in glioblastoma. Based on the described observations we hypothesized that interaction of endothelial cells and glioblastoma cells in the perivascular niche enables stem cell properties in glioblastoma cells and therefore leads to therapy resistance. In the present study we investigated the effect of an *in vitro* co-culture model of endothelial cells and glioblastoma cells and its effect on

(1) **stem cell marker** expression
(2) **clonogenic survival**,
(3) **radioresistance** and
(4) **migration potential**

in glioblastoma cells.

The corroboration of the glioblastoma stem cell hypothesis would have significant clinical implications. In order to prevent tumour recurrence new treatment approaches would have to target this specific subpopulation instead of seeking to eradicate every differentiated tumour cell.

2 Material and methods

2.1 Routine cell culture procedure

Two lines of human endothelial cells and two lines of human glioblastoma cells were used for the experiments described below. Their specifications and management will be described in the following. A tabular overview of the used cell lines, origin and used media can be found in the appendix to this chapter (Table 7).

For initial growth all cells were incubated in 75 or 25 cm^2 flasks with standard conditions (37°C, 5% CO_2, 98% relative humidity). The medium was replaced every three and two days, respectively, after a certain coverage was reached. To detach the cells the medium was discarded and the flasks were washed with 7 ml PBS to remove debris of perished cells and remaining proteins from the FCS. Those would have corrupted the enzymatic detachment. After washing, 1 ml of Trypsin was added and the flasks were incubated for another 5 min. When applied shortly Trypsin degrades extracellular adhesion proteins. This enzymatic reaction was stopped through the addition of 9 ml of FCS-containing medium in which the detached cells were resuspended. To remove trypsin residue the supernatant was removed after centrifugation (1000 rpm, 5 min, room temperature) and the cell pellet was resuspended in fresh media. After counting in a Neubauer counting chamber the cells were brought to further cultivation or directed to an experiment.

For long term storage 10% of DSMO was added to the suspension. After slow precooling at a rate of 1°C/min in a cell freezing container the suspension was stored at -80°C.

2.2 Endothelial cell lines

2.2.1 Human umbilical vein endothelial cells (HUVEC)

Human umbilical vein endothelial cells have kindly been provided by Dr. Petra Fallier-Becker from the department of pathology and neuropathology at the

University of Tübingen. For cultivation of the HUVEC the VascuLife EnGS Kit medium was used.

Table 1: VascuLife EnGS supplements

Substanz	Menge	Endkonzentration
VascuLife Basal Medium	475 ml	
EnGS LifeFactor	1 ml	0.2%
Ascorbic Acid	0.5 ml	50 µg/ml
Hydrocortisone Hemisuccinate	0.5 ml	1.0 µ/ml
FBS	10 ml	2%
L-Glutamine	25 ml	10 mM
rh EGF	0.5 ml	5 ng/ml
Heparin Sulfate	0.5 ml	0.75 units/ml

For ideal adherence and maintenance of the HUVEC's differentiation the flasks were coated with gelatin.

2.2.2 Human cerebral microvascular cells (hCMEC/D3)

The hCMEC/D3 (CELLusions Biosystems, Burlington, Canada) cell line consists of immortalized human endothelial cells derived from microvasculature of the brain. They have been isolated from a resectate of the temporal lobe of the brain acquired during an epilepsy surgery procedure following immortalization via the transfection of the genes *hTERT* and *SV40 large T.*

The EndoGRO-MV Kit medium with the addition of b-FGF (R&D Systems, Minneapolis, USA) at a concentration of 1 ng/ml was used for the cultivation of the hCMEC/D3 cell line as recommended by CELLutions Biosystems.

Table 2: EndoGRO-MV Complete Culture Kit supplements

Substanz	Menge	Endkonzentration
EndoGRO Basal Medium	475 ml	
EndoGRO-LS Supplement	1 ml	0.2%
Ascorbic Acid	0.5 ml	50 µg/ml
Hydrocortisone Hemisuccinate	0.5 ml	1.0 µ/ml
FCS	25 ml	5%
L-Glutamine	25 ml	10 mM
rh EGF	0.5 ml	5 ng/ml
Heparin Sulfate	0.5 ml	0.75 units/ml

hCMEC/D3 cells were cultured in 25 cm^2 flasks. Their culture surface was coated with rat tail collagen according to the instruction leaflet. Cells were seeded at a density of 5,000-20,000 cells per cm^2. After seeding, the hCMEC/D3 cells formed a monolayer until reaching full confluency, which slowed their growth through contact inhibition. Regarding the strong cell-cell-junctions respectively cell-matrix-junctions 2 ml of trypsin were used for one fully confluent 25 cm^2 flask with an incubating time of 10 min after two rinsing steps with PBS.

2.3 Glioblastoma cell lines

2.3.1 T98G

The T98G cell line was isolated from the primary glioblastoma of a 61-year-old male Caucasian. It's characterized by a hyperpentaploid set of chromosomes, anchor-independent growth and immortality with a stationary phase G1 arrest *in vitro* [53]. First of which are typical characteristics of malignant cells. The T98G cells were been cultivated in 10% fetal calf serum supplemented Dulbecco's Modified Eagle's Medium (Sigma Aldrich, St. Louis, USA) according to chapter 2.1.

2.3.2 U87MG Katushka

The U87MG is the most widely used glioblastoma cell model being the basis for over 1700 listed publications over the last four decades, despite its unknown origin[54]. The primary U87MG cells have been purchased from ATCC (Bethesda, Maryland, USA) and have then been transfected with the far-red fluorescent protein TurboFP635-N “Katushka” (BioCat, Heidelberg, Germany) through the transfection agent FUGENE HD (Roche Diagnostics GmbH, Mannheim, Germany) in the Department of Pharmacy, University of Regensburg (see Edalat L. et al.[55]). They also proved that the transfected U87MG Katushka cells were similar to the wild type cells regarding chemosensitivity and growth kinetics [55]. The U87MG Katushka cells were cultivated in 75 cm^2 flasks according to the routine cell culture procedure using 10% FCS-supplemented RPMI-1640 medium (Sigma Aldrich, St. Louis, USA).

2.4 Endothelial-Glioblastoma Co-culture

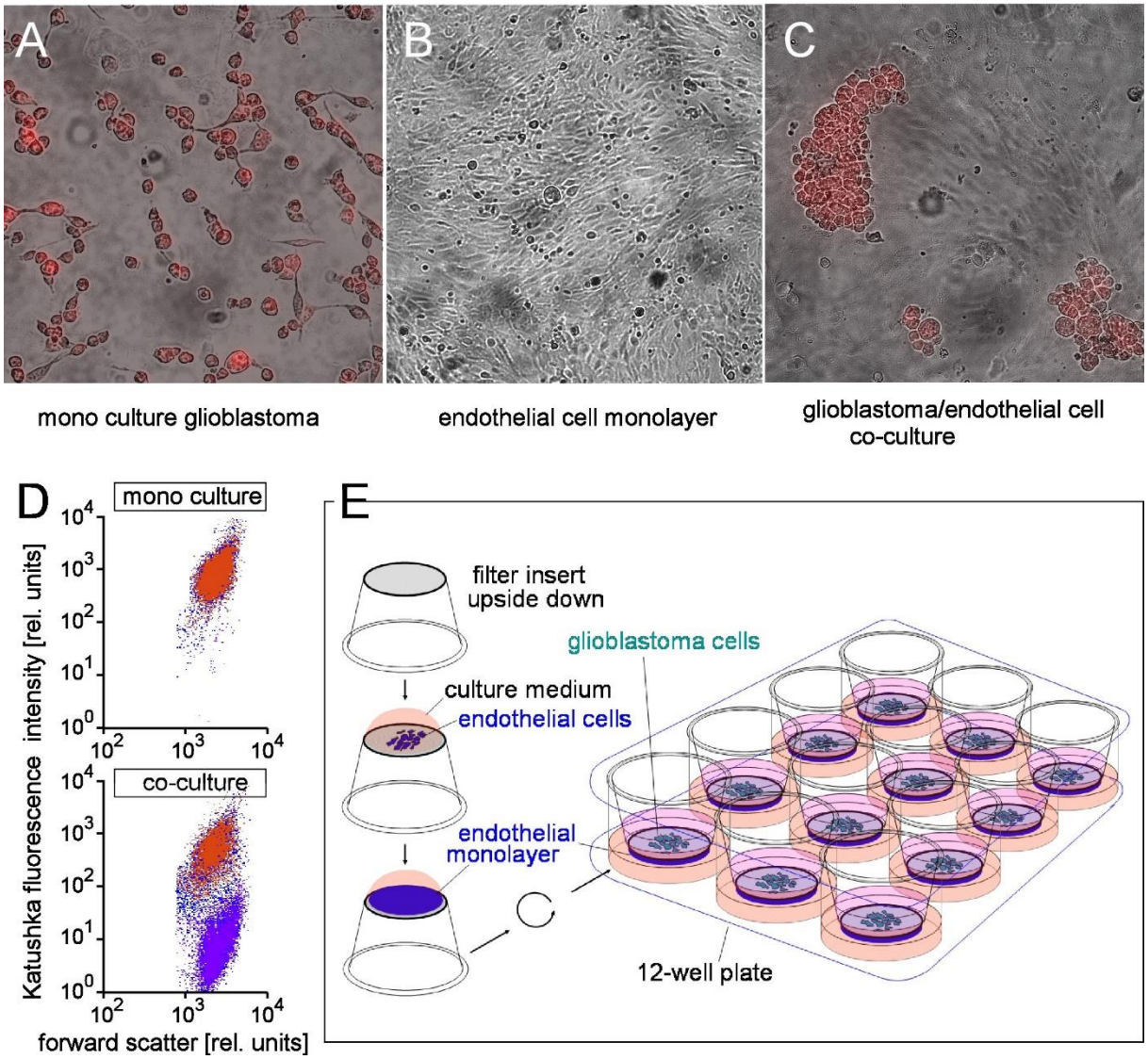

Figure 1. Co-cultures of the human glioblastoma cells and endothelial cells. **A-D**. Direct Co-culturing of the red fluorescent U-87MG-Katushka glioblastoma cells on top of an endothelial cell monolayer. Given are a fluorescence micrograph of the glioblastoma monoculture (A), a light micrograph of an endothelial cell monolayer (B), a superimposed fluorescence/light micrograph of a glioblastoma/endothelial cell co-culture (C) as well as a dot blots (D) showing the Katushka fluorescence and the forward scatter of glioblastoma cells in monoculture (top) and in co-culture with endothelial cells (bottom) as recorded by flow cytometry. **E**. Scheme depicting the filter-separated co-culturing of endothelial cells with human U-87MG-Katushka or T98G glioblastoma cells.

2.4.1 Direct contact co-culture

A direct co-culture approach as shown in **Figure 1**C describes a technique where Glioblastoma cells and endothelial cells were cultured in the same culture volume and medium with the endothelial cells forming a monolayer on the bottom and the glioblastoma cells growing adherently to this monolayer. This approach was used for experiments where direct cell-cell-contact was needed for data acquisition e.g. immunofluorescence or experiments where the two cell lines could easily be separated e.g. flow cytometry (see **Figure 1**D). It allows a close cell communication via cell-cell-junctions and paracrine signalling.

For the direct co-culture either 6-well plates or 25 cm^2 flasks were used. For better adhesion and stable differentiation, the culture surface was coated with gelatine extracted from bovine skin following the manual of the provider (Table 9. Cell culture substances). After coating, the respective endothelial cells were seeded and grown until complete confluency whereby the media was changed regularly. After reaching full confluency the medium was discarded and glioblastoma cells were overlaid in a suspension in fresh endothelial medium with a cell density ranging from 2500 to 3000 cells per cm^2. After 24 or 72 h of coculturing the glioblastoma cells were harvested. To this end, 0,.1 ml of Cell Dissociation Buffer (CDS, Millipore, Darmstadt, Germany) per cm^2 was incubated for 6 min which resulted in the detachment of the glioblastoma but not of the endothelial cells.

2.4.2 Indirect co-culture

For experiments where a better separation of endothelial cells and glioblastoma cells was required, e.g. colony formatting assays and RNA analyses, an indirect co-culture approach was used. Therefore, 6-well plates were coated with gelatine and overgrown with an endothelial cell monolayer as described before. Instead of directly adding the glioblastoma cell suspension into the wells it was pipetted into a cell culture insert with a 3 µm pore sized membrane that was placed inside the wells. This allowed paracrine cell signalling and an easy and safe separation of the different cell lines.

2.4.3 Transfilter co-culture

A progression of the indirect co-culture is the transfilter co-culture, which was used for the majority of the experiments. In this approach the endothelial cells and the glioblastoma cells grow on either side of the membrane of a cell culture insert (see **Figure 1**E). Its 3 µm pores allow not only paracrine but also direct cell-to-cell-communication through cellular protrusions in the pores.

For this technique the cell culture inserts were turned upside down. The now upward-facing side of the membrane was coated with a collagen solution derived from rat tails according to the distributor's manual, which included one hour of incubating and double rinsing the coated membrane off the alkaline solution with PBS. Then 1 ml of a hCMEC/D3 endothelial cell suspension with a cell density of 10000 cells/ml was pipetted on the upward-facing, collagen-coated side of the insert's membrane. The cells were allowed to sediment and adhere for 12 h in the incubator after which the media was carefully removed with a pipette. Next, the inserts were flipped again and placed inside the wells of a 6-well-plate. The wells outside of the inserts were filled with 3 ml of the endothelial medium. The endothelial cells were incubated for another 48 h to reach full confluency and attachment. Then the insides of the inserts were filled with 2 ml of a glioblastoma cell suspension containing 20,000 to 130,000 cells in endothelial medium and the medium in the well outside the insert was changed. This co-culture environment was incubated for 48-96 h following treatment and harvesting the glioblastoma cells. Therefore, the insert was transferred to a new 6 well plate. The medium from the insides of the inserts was collected in a 10 ml falcon, the insert was carefully rinsed with 1 ml of PBS, which was collected, too. Then 0.5 ml of trypsin was added for cell detachment and the inserts incubated for 5 min at 37°C. The enzymatic reaction of the Trypsin was stopped with the addition of 2 ml 10% FCS supplemented glioblastoma medium, both were collected in the falcon, centrifuged at 1000 rpm for 5 min. The supernatant was discarded and the cell pellet was directed to analysis and experiments.

2.5 Irradiation

Cells were irradiated with 6 MV photons using the linear accelerator LINAC SL25 Philips at the Department of Radiooncology at the University Hospital Tübingen. Irradiation took place at room temperature with a dose rate of 4 Gy/min.

2.6 SDF-1 Immunofluorescence microscopy

2.6.1 Concept

Immunofluorescence visualizes the distribution and quantity of biomolecules present in *in vitro* cell cultures or tissue samples. Therefore, specific antibodies bind the investigated molecule in fixed cells and are bound by another less specific antibody conjugated with a fluorophore in a second step. Pictures are then obtained with light microscopy in combination with a suitable excitation light source.

2.6.2 Procedure (modified from Edalat, Stegen, Klumpp, Haehl et al., [55])

U-87MG Katushka cells and HUVEC were grown in a direct co-culture approach (see 2.4.1) for 24 h on Millicell EZ object slides (Millipore, Darmstadt, Germany). *“Then, cells were fixed for 15 min at room temperature with phosphate buffered saline (PBS)containing 4% formaldehyde, 3 times rinsed with PBS for 5 min and blocked for 1 h at 21°C with PBS additionally containing 1% bovine serum albumin (BSA), 5% goat serum and 0.3% Triton X-100. Cells were then incubated with polyclonal rabbit anti-SDF-1 antibody (Novus Biologicals, R & D Systems Europe, Abingdon, UK) or rabbit IgG isotype control antibody (Merck-Millipore, both 1 mg/ml) diluted (both 1:1000) in PBS containing 1% BSA and 0.3% Triton X-100. Thereafter, cells were rinsed 3 times for 5 min with PBS, incubated for 2 h at room temperature in the dark with goat FITC-conjugated anti-rabbit IgG antibody (1:1000, NB730-F, Novus Biologicals) diluted in PBS/1% BSA/0.3% Triton X-100, rinsed 3 times for 5 min with PBS, and*

coverslipped with 4',6-diamidino-2-phenylindole (DAPI) Vectashield Antifade Mounting Medium (Vector Laboratories, Loerrach, Germany)." [55] Micrographs were obtained with an inverted Axiovert Zeiss fluorescence microscope.

2.7 Colony formation assay

2.7.1 Concept

The colony formation assay is a well-established and widely used *in vitro* tool to investigate survival and the capability of proliferation of large cell populations facing certain treatments or environments. It analyses the number of colonies originating from a known number of singularized cells being grown under set conditions by staining and counting, following a certain treatment or exposure. The comparison of the results from different environmental factors or treatments allows drawing conclusions about the influence of these on cell damage and the capability of proliferating. If used with cancer-derived cells the colony formation assay may indicate vulnerability or treatment response of these cancer entities to the tested procedures.

2.7.2 Procedure

Filter-separated glioblastoma and endothelial cells were co-cultured as described in 2.4.2. and 2.4.3. After coculturing and irradiation the cells were incubated for another 24 h. Then, the inserts containing the treated glioblastoma cells were transferred to a new 6-well plate, the medium was discarded and the cells were carefully rinsed with 1 ml of PBS. 0.5 ml of trypsin was added per insert and incubated at 37°C for 5 min. The proteolytic effect of trypsin was stopped by the addition of 2 ml of medium, the suspension was centrifuged at 1000 rpm for 5 min, the supernatant discarded and the pellet resuspended in another 10 ml of glioblastoma medium. After counting and corresponding dilution, 300 cells in 2 ml glioblastoma medium were plated in each well of a 6-well plate. The cells were incubated for 2-3 weeks at standard conditions to allow colony formation.

After that given time the medium was discarded and 3 ml of a 3.7% solution of formaldehyde per well was added for 10 min. Next 3 ml of a 10% ethanol solution was added for another 10 min. The hence fixed cells were rinsed with pure water and 3 ml of a 0.05% Coomassie (20% methanol, 7.5% acetic acid, 72.5% pure water, 0.5 g Brillant Blue R-250) solution was added for colour staining. After 15 min the 6-well plates were rinsed again with pure water and left for drying.

The number of colonies as defined by cell clusters of 50 or more cells, were counted for every well using a stereo microscope.

The plating efficiency was defined by dividing the number of colonies by the number of plated cells. Survival fractions were calculated by dividing the plating efficiency of the irradiated cells by those of the unirradiated controls and fitted by the use of the linear-quadratic equation [55].

2.7.3 Treatment

Seven independent colony formation assays were performed during this work testing the radiation (0, 2, 4 or 6 Gy)-dependent clonogenic survival of glioblastoma cells growing in monocultures against glioblastoma cells growing in an endothelial co-culture. For the first three colony formation assays the T98G cell line was used with an indirect co-culture approach (see Indirect co-culture 2.4.2). The duration of co-culturing was 48-72 hours and 10,000 T98G cells were added per insert. For another four colony formation assays, the U-87MG Katushka cell line was used with the transfilter co-culture approach (2.4.3).

During the course of the latter series of experiments, plated cell number (10,000 – 100,000 cells per insert), FCS concentration (2,5% - 10%) and beta-FGF concentration (0 - 1 ng/ml) were adapted. In one experiment irradiation was administered in a daily fractioned scheme. These adaptions had no effect on plating efficiencies or survival fractions. Therefore, these data were pooled.

Table 3: Colony formation assays

	GB cell line	Endothel	Co-culture	time	Additional information
CFA1	T98G	HUVEC	indirect	48 h	
CFA2	T98G	HUVEC	indirect	72 h	
CFA3	T98G	HUVEC	indirect	72 h	
CFA4	U87MG Kat	hCMEC/D3	transfilter	48 h	
CFA5	U-87MG Kat	hCMEC/D3	transfilter	72 h	Fractioned irradiation
CFA6	U-87MG Kat	hCMEC/D3	transfilter	72 h	Beta-FGF depletion
CFA7	U-87MG Kat	hCMEC/D3	transfilter	96 h	FCS-reduction

2.8 Flow cytometry

2.8.1 Concept

Flow cytometry is a high throughput method that exposes single cells to laser light and measures the emitted light. These readouts include fluorescence emission light at different wavelengths and forward as well as sideward scatter – the latter two as a measure of cell size and granularity, respectively. Three different agents were used. The far-red fluorescent protein Katushka expressed by the U87MG cells was used to differentiate endothelial cells and glioblastoma cells. Annexin-V-fluos (Roche Life Science, Mannheim, Germany) and CaspACE FITC VAD-FMK (Promega, Madison, USA) were used as markers for apoptotic cells [56-58]. FITC-Annexin V detects the breakdown of the phospholipid asymmetry of the plasma membrane, whereas VAD-FMK is a cell permeable caspase inhibitor that binds to activated caspases. Both agents were conjugated with the fluorochrome fluorisothiocyanat (FITC).

2.8.2 Procedure

The flow cytometry analyses were performed on an FACS Calibur (Becton Dickinson, Heidelberg, Germany). After harvesting the cells the suspension was added into special vials suitable for the flow cytometer, centrifuged at 1200 rpm for 4 min, the supernatant carefully taken off and the cell pellet resuspended in 200 µl NaCl solution (in mM: 125 NaCl, 32 N-2-hydroxyethylpiperazine- N -2-

ethanesulfonic acid (HEPES), 5 KCl, 5 D-glucose, 1 MgCl2, 1 CaCl2, titrated with NaOH to pH 7.4) supplemented with the respective fluorescent agent. Annexin V was used in a 1:250 dilution and CaspACE in a concentration of 5 µM. Both were incubated for 30 min at room temperature. The cell samples were exposed to blue (488nm) and red (635nm) light and emissions were recorded at 661 nm (FL3-H) to gate the Katushka-positive cells [59, 60] and at 530 nm (FL1-H) to assess the Annexin V and CaspACE specific fluorescence [61]. Annexin V and CaspACE specific fluorescence was then determined by analysing FL-1 positivity in Katushka fluorescent (FL-3 positive) gated cells. Data were analyzed with the FCS Express 3 software (De Novo Software, Los Angeles, CA, USA).

2.8.3 Treatment

T98G and U-87MG Katushka cells were either grown in direct co-culture (see 0) with HUVEC and hCMEC/D3 endothelial cells or in monoculture. Prior to flow cytometry cells were irradiated with doses of 0 or 6 Gy and then analysed by Annexin V and CaspACE assay 24 h thereafter.

2.9 Quantitative RT-PCR

2.9.1 Concept

The quantitative RT-PCR in combination with reverse transcription is a tool to analyse the concentration of cellular messenger RNA. mRNA expression is subject to a variety of short term modulations as a way to adapt to environmental stimuli. For a quantitative approach the relative results of mRNA expression need to be compared to the, per definition moderately stable, concentration of housekeeper genes mRNA.

2.9.2 Procedure and primers

Messenger RNA was isolated from the cells using RNA extraction kit form Quiagen (Hilden, Germany). RNA amount and purity was analysed with a NanoDrop 1000 (NanoDrop Technologies, Wilmington, USA). For reverse

transcription and template amplification two different techniques were used, whereby amplification was always performed in a Roche LightCycler (Mannheim, Germany). For the majority of the analyses the isolated mRNA was reversely transcribed into cDNA using the Transcriptor First-strand cDNA Synthesis kit by Roche on a Mastercycler personal (Eppendorf, Hamburg, Germany). Amplification was performed using the Quanti Fast SYBR Green PCR Kit by Quiagen on the Roche LightCycler. Further analyses were performed using the single-step Rt qPCR Green ROX L Kit by highQu (Kraichtal, Germany) for transcription and amplification by the LightCycler after RNA isolation. Primers from the QuantiTect Primer Assay by Quiagen were used for amplification. Those were specific for von-Willebrand-factor, Prominin-1, MSI-1, Nestin, Sox2, Oct4, Notch-1, KCNN4, KCNMA1, TRPM8, CXCR4, SDF-1, MMP-2, MMP-9, TGF-beta receptor-1, TGF-beta-1 and housekeepers β-actin, glyceraldehyde-3-phosphate dehydrogenase, and pyruvate dehydrogenase beta (see Table 4).

Table 4: Primers used for qPCR

Primer	Description or Synonym	Gen-class	Catalogue number
vWF	Von-Willebrand-factor	endothelial marker	QT00051975
CD133	Prominin-1	stem cell marker	QT00075586
MSI-1	Musashi-1	stem cell marker	QT00025389
Nestin		stem cell marker	QT00235781
Sox2		stem cell marker	QT00237601
Notch-1		stem cell marker	QT01005109
Oct4	POU5F1	stem cell marker	QT00210840
KCNN4	IK	ion channel	QT00003780
KCNMA1	BK	ion channel	QT00024157
TRPM8		ion channel	QT00038906
CXCR4		chemokine-receptor	QT00223188
SDF-1	CXCL12	chemokine	QT00087591
MMP-2		matrix-metalloprotease	QT00088396
MMP-9		matrix-metalloprotease	QT00040040
TGF-beta receptor-1		growth factor-receptor	QT0008412
TGF-beta-1		growth factor	QT00000728
ACTB	β-actin	housekeeper	QT00095431
GAPDH	glyceraldehyde-3-phosphate dehydrogenase	housekeeper	QT01192646
PDHB	pyruvate dehydrogenase beta	housekeeper	QT00031227

2.9.3 Treatment

Quantitative RT-PCR analyses were performed using T98G and U-87MG Katushka cell lines. They were conducted with either the direct co-culture approach, using CDS for detaching the cells where a visually intact endothelial layer was remaining, or the transfilter co-culture approach, with the use of trypsin for cell harvesting.

5 independent quantitative RT-PCR analyses were performed using the T98G and U-87MG Katushka cell lines. Two experiments were conducted with the direct co-culture approach (0). Here, cells were detached under visual control using CDS where the endothelial monolayer remained intact. The remaining 3 experiments were performed with the transfilter co-culture approach (2.4.3) with the use of trypsin for cell harvesting. Data for direct and transfilter co-culture were pooled separately.

Table 5: Quantitative RT-PCR

	GB Cell-line	Endothelium	Co-culture-	-time	Irradiation
RT-PCR1	U-87MG Kat	hCMEC/D3	direct	96h	5x2Gy
RT-PCR2	U-87MG Kat	hCMEC/D3	direct	24h	5x2Gy
RT-PCR3	U-87MG Kat	hCMEC/D3	transfilter	96h	5x2Gy
RT-PCR4	U-87MG Kat	hCMEC/D3	transfilter	96h	5x2Gy
RT-PCR5	U-87MG Kat	hCMEC/D3	transfilter	48h	5x2Gy

2.10 Patch-clamp recording

2.10.1 Concept

The patch-clamp technique is an electrophysiological method to record membrane potential and the activity of electrogenic membrane transports, especially through ion channels, in living cells. From the variety of methods the on-cell/cell-attached approach was used in the present work. Hereby, the micrometer-sized tip of a glass pipette is attached to the surface of a living cell by suction without destroying the integrity of the cell membrane as a whole. Single or small numbers of transmembrane proteins and ion channels of this

isolated membrane patch can now be examined. The pipette and bath solutions resemble the interstitial space. The bath solution is continuously superfused and its chemical composition can be changed during recording. With the voltage clamp method the transmembrane currents are measured at different clamped transmembrane voltages, thus retrieving current-voltage-curves for the recorded membrane area. Those curves allow to draw conclusions about the different ion-channel activities.

2.10.2 Procedure (modified from Edalat, Stegen, Klumpp, Haehl et al., [55])

"On-cell currents were evoked by 41 voltage square pulses (700 ms each) from" 0 mV "holding potential to voltages between" -100 and +100 mV "delivered in 5 mV increments." "*Applied voltages refer to the cytoplasmic face of the membrane with respect to the extracellular space." "Cells were superfused at 37°C temperature with NaCl solution (in mM: 125 NaCl, 32 N-2-hydroxyethylpiperazine- N -2-ethanesulfonic acid (HEPES), 5 KCl, 5 D-glucose, 1 MgCl2, 1 CaCl2, titrated with NaOH to pH 7.4)" [55].* The same solution was used in the pipette. Borosilicate glass pipettes (~5 MΩ pipette resistance; GC150 TF-10, GC150 TF-10, Harvard Apparatus, March-Hugstetten, Germany) manufactured by a microprocessor-driven DMZ puller (Zeitz, Augsburg, Germany) were used in combination with a STM electrical micromanipulator (Lang GmbH and Co KG, Germany). Currents were recorded with a10 kHz sampling rate and 3-kHz low-pass-filtered by an EPC-9 amplifier (Heka, Lambrecht, Germany) using Pulse software (Heka) and an ITC-16 Interface (Instrutech, Port Washington, NY, USA). Voltage-dependent open probability of an undefined number n of channels in the sealed patch (nPo) was calculated by dividing the calculated difference between averaged macroscopic current and the physical leak current (i. e., the averaged current minimum at no apparent channel activity) by the channel amplitude.

Macroscopic on-cell currents were analyzed by averaging the currents between 100 and 700 ms of each square pulse. Outward currents, as the flow of positive charge (here: K+) from the cytoplasmic to the extracellular membrane face, were

technically defined as positive currents. For single-channel recordings continuous holding potentials were applied.

2.11 Migration assay

2.11.1 Concept

With the migration assay performed in the present work, the capability of cells to migrate following a chemotactic gradient can be observed in real-time. After treatment, cells were plated on the upper *cis* side of a filter insert array. The cis side of the filter contained a lower concentration of a chemoattractant as compared to the lower *trans* side chamber. The electric impedance was continuously recorded between gold electrodes vapour deposited at the *trans* side of the filter and reference electrodes situated at the bottom of the lower chamber. Trans-filter chemotaxis of the cells followed by cell attachment on the electrode surface at the *trans* side of the filter resulted in an increase in impedance which allows the real-time monitoring of transfilter chemotaxis.

2.11.2 Procedure

For all migration assays the U-87MG Katushka glioblastoma cells and the hCMEC/D3 endothelial cell line for coculturing were used with the filter separated coculturing approach (2.4.3). The assays were performed using CIM-Plates 16 by Roche (Mannheim, Germany) on an xCELLigence RTCA DP (ACEA Bioscience, San Diego, USA) under standard conditions in an incubator. Prior to the assay, the cells were co-cultured using the transfilter approach (2.4.3) for 48 to 96 h with 50,000 to 130,000 glioblastoma cells per insert. Following treatment, the cells were harvested as described in 2.4.3, counted and diluted in 1% FCS supplemented RPMI-1640 medium. The lower (*trans* side) and the upper chamber (*cis* side) of the CIM plate were prefilled with 160 µl of 5% FCS supplemented and 100µl of 1% FCS supplemented RPMI-1640 medium, respectively. The plate was equilibrated at standard conditions (37°C

and 5% CO2) for 60 min and the impedance reset to zero. Then 100 µl of the cell suspension containing 40,000 cells were added to the upper chamber (*cis* side). After cell sedimentation and adherence, the migration was analysed in real-time by measuring the impedance between the electrodes every 5 min. for 24 h.

2.11.3 Treatment

Table 6: Migration assays

	GB cell line	**Endothelium**	**Co-culture-**	**-time**
MA1	U-87MG Kat	hCMEC/D3	transfilter	48h
MA2	U-87MG Kat	hCMEC/D3	transfilter	72h
MA3	U-87MG Kat	hCMEC/D3	transfilter	96h
MA4	U-87MG Kat	hCMEC/D3	transfilter	48h
MA5	U-87MG Kat	hCMEC/D3	transfilter	72h
MA6	U-87MG Kat	hCMEC/D3	transfilter	72h
MA7	U-87MG Kat	hCMEC/D3	transfilter	96h
MA8	U-87MG Kat	hCMEC/D3	transfilter	72h

8 independent migration assays were performed on cells that were grown in monoculture or filter separated co-culture.

3 Results

To disclose interactions between glioblastoma and endothelial cells human far-red fluorescent U-87MG-Katushka glioblastoma cells and human T98G glioblastoma cells were co-cultured with human endothelial cells. Different experiments were carried out using direct co-culture and transfilter co-culture (3 µM pore size) that carry an endothelial cell monolayer on the opposite filter face. Hereby human umbilical vein endothelial cells (HUVEC) were used for initial experiments and human cerebral microvascular endothelial (hCMEC/D3) cells for later ones to achieve a closer resemblance to the physiological setting.

3.1 Co-culture with HUVEC (Human umbilical vein endothelial cells)

3.1.1 SDF-1 Immunofluorescence

The effect of endothelial cell co-culturing on SDF-1 abundance in glioblastoma cells was analysed on protein level by immunofluorescence microscopy in direct U-87MG-Katushka/endothelial cell (HUVEC) co-cultures (24 h co-culture time) and monocultures grown on object slides. **Figure 2** A-C shows the (immuno-)reactivity of DNA (DAPI, blue), Katushka protein (red), SDF-1 protein (green, A, B) and of that elicited by the unspecific binding of an IgG isotype antibody used to control the specificity of the SDF-1 antibody (green, C). The data suggest similar SDF-1-specific immunoreactivity in the nucleus and cytoplasm of mono- and co-cultured U-87MG-Katushka cells. In addition, Katushka-negative endothelial cells exhibited a high cytoplasmic and perinuclear SDF-1-specific immunoreactivity (**Figure 2** D). Semi-quantitative analysis of the cytoplasmic SDF-1-specific immunoreactivity shows significantly higher SDF-1 abundance in endothelial cells as compared to U-87MG-Katushka cells (quantified mean 7.54 vs. 5.45; relative units; $p<0.01$), but no significant difference between mono- or co-cultured glioblastoma cells (5.00 vs. 5.70; relative units; $p=0.37$). Combined, the data on SDF-1 protein do not show an endothelial cell-induced increase in SDF-1 mRNA abundance in glioblastoma cells.

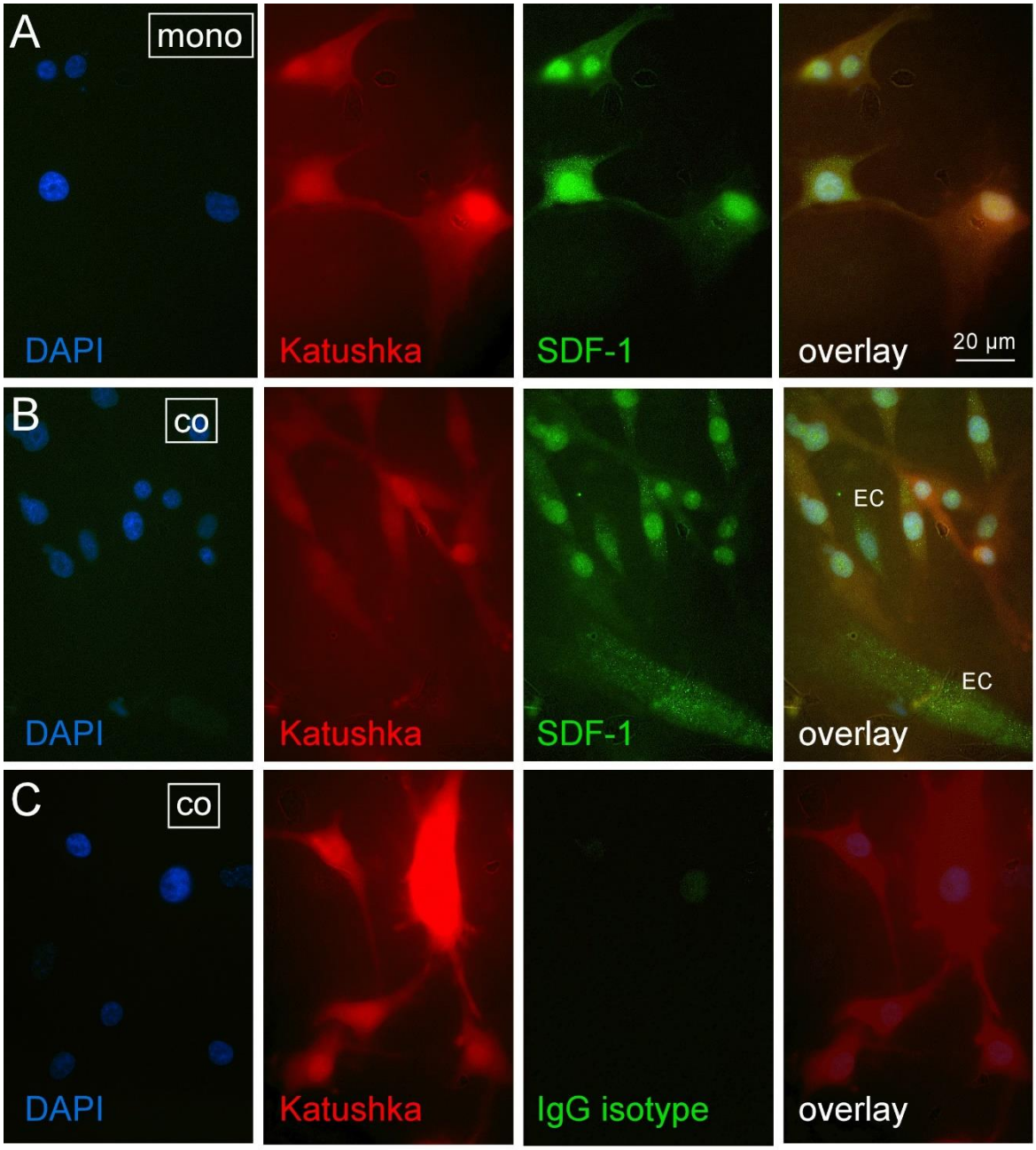
A
mono
DAPI
Katushka
SDF-1
overlay
20 µm
B
co
DAPI
Katushka
SDF-1
EC
EC
overlay
C
co
DAPI
Katushka
IgG isotype
overlay
D
co
EC
DAPI
Katushka
SDF-1
EC
EC
EC
10 µm
E
*
SDF-1-specific fluorescence intensity [rel. units]
0
2
4
6
8
U-87MG-Katushka
U-87MG-Katushka
endothelial cells
mono-
co-culture

Figure 2. Endothelial (HUVEC) and U-87MG-Katushka glioblastoma cells express SDF-1 protein. **A-C.** Fluorescence micrographs of U-87MG-Katushka cells grown in monoculture (A) or direct co-culture with endothelial cells (B-C) showing DAPI-stained nuclei (blue, outer left), Katushka protein (red, middle left), SDF-1 protein (A-B, green, middle right), or staining elicited by an unspecifically bound IgG isotype control antibody (C, green, middle right), or all three fluorochroms in overlay (outer right). **D.** Overlay of DAPI- (blue), Katushka- (red), and SDF-1 (green)-specific fluorescence micrographs of a direct U-87MG-Katushka/endothelial cell co-culture in higher power. **E.** Quantified mean (± SE, n = 62-111 cells) SDF-1-specific fluorescence intensity of U-87MG-Katushka cells in monoculture (white), U-87MG-Katushka cells in direct co-culture with endothelial cells (black), and endothelial cells in direct co-culture with U-87MG-Katushka cells (green). * indicates $p \leq 0.05$, Kruskal-Wallis test (nonparametric ANOVA) and Dunn's Multiple Comparisons post test.

3.1.2 Flow cytometry

The effect of hCMEC/D3 endothelial cells on radiation-induced cell death of U87MG-Katushka glioblastoma cells was studied by flow cytometry (direct co-culture, 24 h co-culture time). The two cell lines were well separable by the far-red Katushka fluorescence (**Figure 3**A). Mean percentage of Annexin V positive cells was 9.7% and 7.5% for non-irradiated mono- and co-cultured glioblastoma cells and 14.3% and 18.5% for irradiated glioblastoma cells, respectively. There was no significant difference between mono- and co-cultured glioblastoma cells, but a highly significant difference between irradiated and non-irradiated cells ($p<0.01$) (**Figure 3**B). This showed a radiation induced break-down of the phospholipids asymmetry of the plasma membrane, as a marker of increased apoptosis.

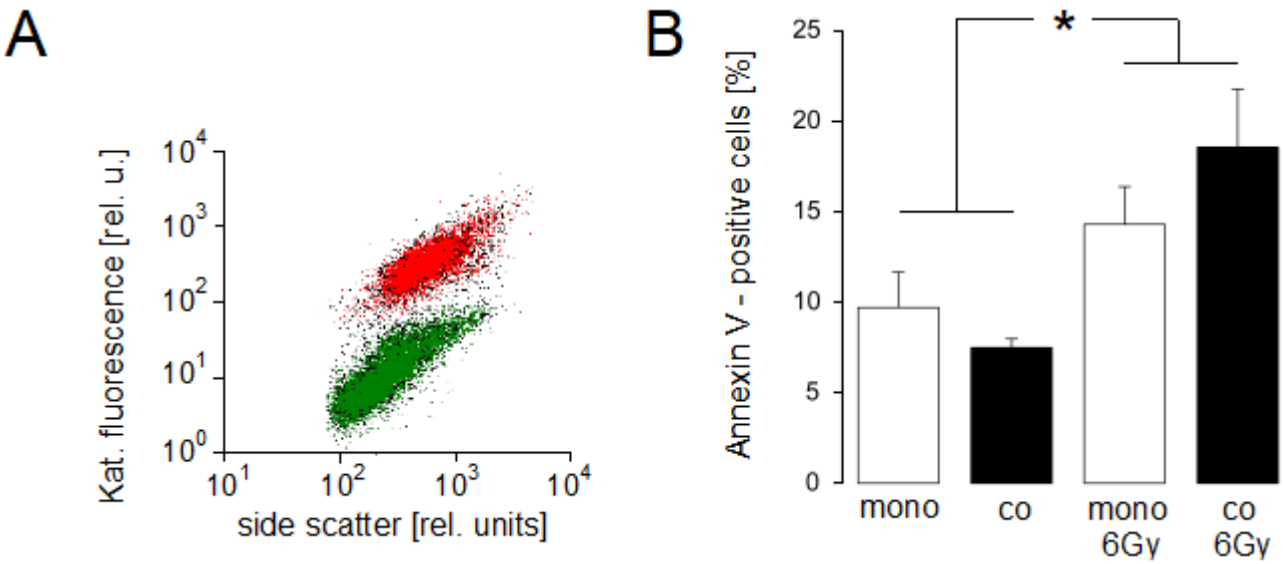

Figure 3 Endothelial cells (HUVEC) have no protective or radiosensitizing effect on apoptotic cell death of U-87MG-Katushka cells. **A.** Dot blots plotting the Katushka fluorescence against the side scatter as recorded by flow cytometry in direct U-87MG-Katushka/endothelial cell (hCMEC/D3) co-cultures. **B.** Mean (± SE, n = 8) Annexin V fluorescence intensity of U-87MG-Katushka cells (as recorded in A) grown in monoculture (open bars) or direct U-87MG-Katushka/endothelial cell co-culture (closed bars) with or without single-time radiation of 6 Gy. * indicates $p \leq 0.01$, two-tailed (Welch corrected) t-test.

3.1.3 Colony formating assay

The effect of the HUVEC endothelial cells on clonogenicity and radioresistance of T98G glioblastoma cells was studied by delayed plating colony formation assays after an indirect co-culture technique (24 – 72h co-culture time). Neither clonogenic survival as deduced from the plating efficiencies nor radioresistance as deduced from the survival fractions of T98G glioblastoma cells in delayed plating colony formation assays were altered significantly by endothelial cell co-culture. Plating efficiency was 0.098 and 0.115 for mono- vs. co-cultured glioblastoma cells (n=54, p=0.07). Mean survival fractions for 2, 4 and 6 Gy were 0.63 vs. 0.61, 0.39 vs. 0.38 and 0.19 vs. 0.16 for mono- vs. co-cultured glioblastoma cells, respectively (n=54, p values: 0.71, 0.89 and 0.16), **Figure 4**.

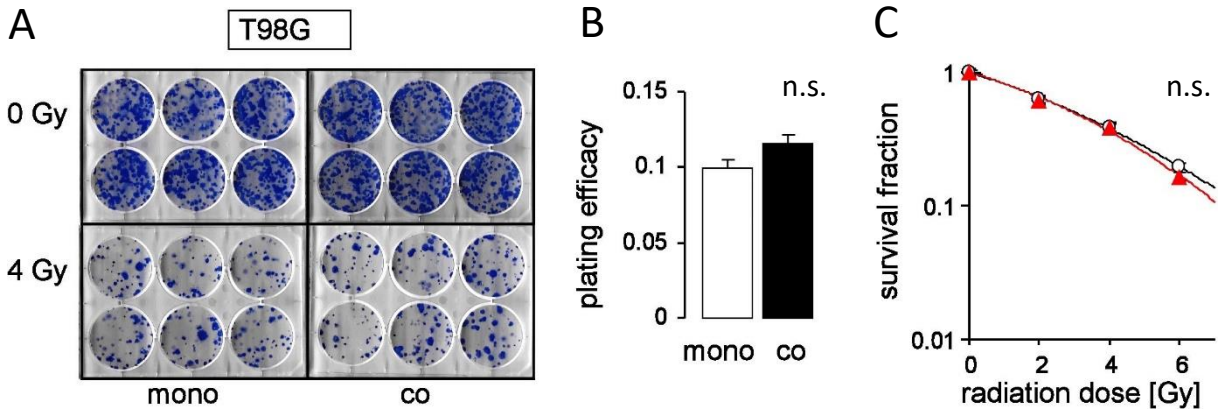

Figure 4. Endothelial cells (HUVEC) do not alter congenic survival or radioresistance of T98G cells. **A** 6-well scans showing Coomassie-stained colonies formed from 300 plated control (0 Gy) or irradiated (4 Gy) cells. **B-C** mean (± SE, n = 54) plating efficacy and mean survival fractions at different radiation dose of T98G cells grown in monoculture (open bars and symbols) or in filter-separated co-cultures with endothelial cells (closed bars and red symbols).

3.2 Co-culture with hCMEC/D3 (human cerebral microvascular endothelial cells)

3.2.1 Flow cytometry

The effect of hCMEC/D3 endothelial co-culture on radiation induced cell death of glioblastoma cells was studied by flow cytometry (direct co-culture, 24 h co-culture time). Radiation significantly increased the apoptotic cell fraction, measured as caspace activation (**Figure 5A**), but no significant effect of the endothelial co-culture on radiation induced cell death could be shown (**Figure 5**B). Mean percentage of CaspACE positive cells was 5.3% and 6.1% for non-irradiated mono- and co-cultured glioblastoma cells and 9.6% and 12.6% for irradiated glioblastoma cells, respectively. There was no significant difference between mono- and co-cultured glioblastoma cells, but a highly significant

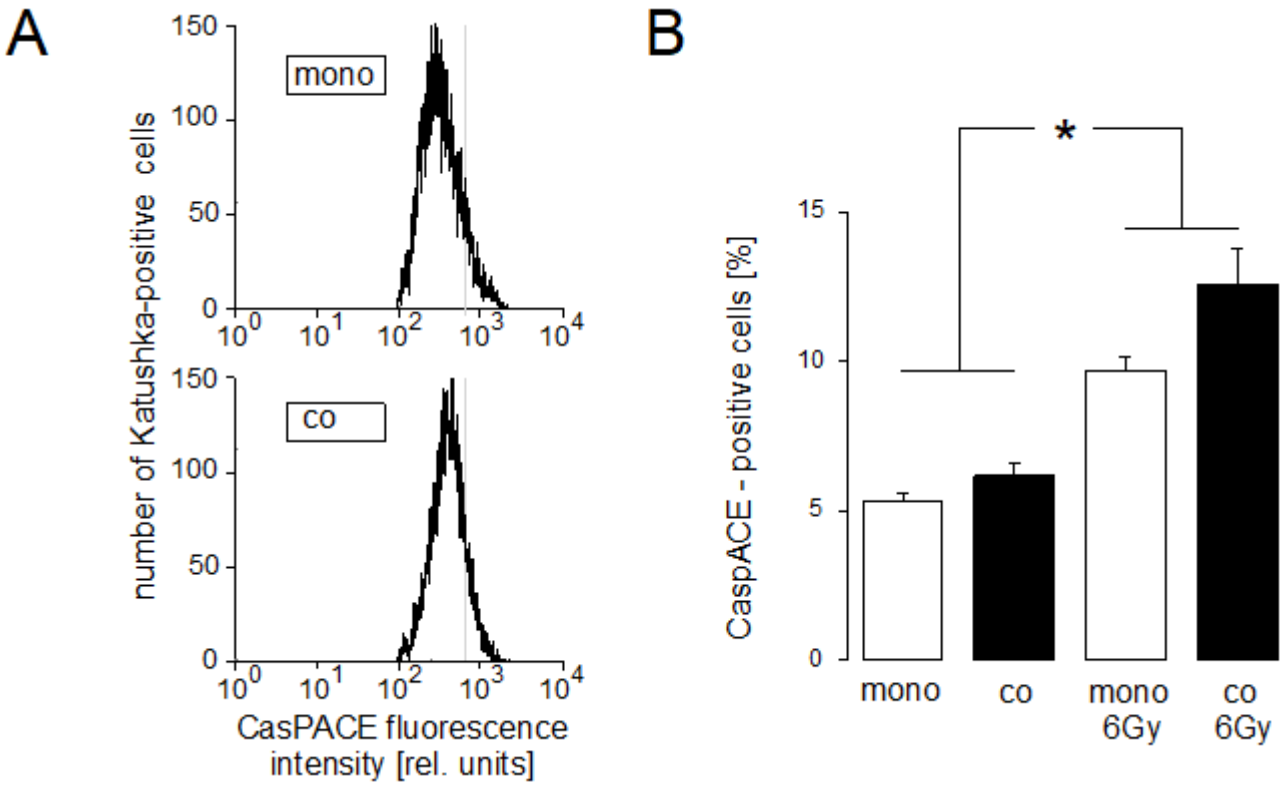

Figure 5. Endothelial cells (hCMEC/D3) co-culture does not alter radiation induced cell death. **A.** Histograms depicting the CasPACE fluorescence of Katushka-positive cells as recorded by flow cytometry in U-87MG-Katushka monocultures (top) and direct U-87MG-Katushka/endothelial cell (hCMEC/D3) co-cultures (bottom). **B.** Mean (± SE, n = 6-8) CasPACE fluorescence intensity of U-87MG-Katushka cells (as recorded in A) grown in monoculture (open bars) or direct U-87MG-Katushka/endothelial cell co-culture (closed bars) with or without single-time radiation of 6 Gy. * indicates $p \leq 0.01$, two-tailed (Welch corrected) t-test.

difference between irradiated and non-irradiated cells ($p<0.01$).

3.2.2 Colony formating assay

In addition to 3.1.2, the effect of endothelial co-culture on clonogenicity and radioresistance was studied on the U87MG Katushka cell line in a transfilter co-culture (48 - 96 h co-culture time) with the human cerebral microvascular endothelial cells (hCMEC/D3) by delayed plating colony formation assays, too. Again, neither clonogenic survival as deduced from the plating efficacies nor radioresistance as deduced from the survival fractions in delayed plating colony formation assays were altered. Plating efficiency was 0.109 and 0.105 for mono- vs. co-cultured glioblastoma cells (n=54, p=0.07). Mean survival fractions for 2, 4 and 6 Gy were 0.74 vs. 0.63, 0.45 vs. 0.37 and 0.16 vs. 0.15 for mono- vs. co-cultured glioblastoma cells, respectively (n=54, p values: 0.07, 0.09 and 0.72),

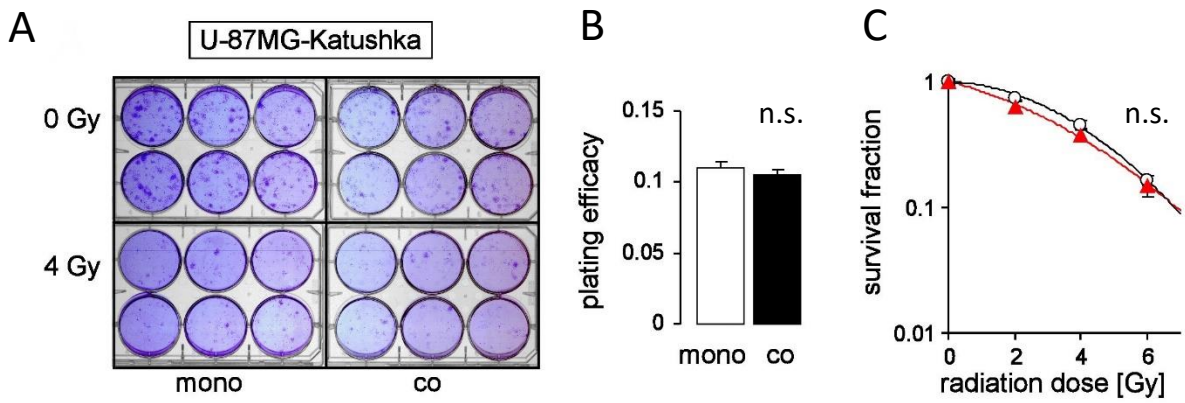

Figure 6. Endothelial (hCMEC/D3) co-culture does not alter clogenic survival or radioresistance of U-87MG-Katushka and T98G cells. A 6-well scans showing Coomassie-stained colonies formed from 300 plated control (0 Gy) or irradiated (4 Gy) cells. B-C mean (± SE, n = 54) plating efficacy and mean survival fractions at different radiation dose of U-87MG-Katushka cells grown in monoculture (open bars and symbols) or in filter-separated co-cultures with endothelial cells (closed bars and red symbols).

(**Figure 6**).

3.2.3 Reveres Transcription Polymerase Chain Reaction

To test for stem cell marker expression and to screen for a variety of possible stem cell properties messenger RNA abundances of U87-MG Katushka glioblastoma cells co-cultured (direct co-culture, 24 - 96 h co-culture time) with hCMEC/D3 endothelial cells were analysed by RT-PCR. In particular, the influence of the endothelial cells on stem cell markers, on ion channels that confer cell migration and/or radioresistance, on SDF-1 (CXCL12)/CXCR4 chemokine signalling, and on matrix metalloproteinases as well as on TGF-beta signalling was analyzed on mRNA level. Co-culture was conducted with the direct and the transfilter technique. To screen for contamination of the glioblastoma cells with endothelial cells, mRNA encoding the endothelial von-Willebrand-Factor (vWF) was compared between glioblastoma mono- and co-cultures and endothelial monocultures. As shown in **Figure 7**A, vWF mRNA abundance was very low in mono- and co-cultured glioblastoma as compared to that of endothelial monocultures suggesting low and insignificant contamination of co-culture glioblastoma cells after separation.

As a result of the RT-PCR experiments, co-culturing with endothelial cells did not significantly affect Prominin-1, Musashi-1, Nestin, Notch, Sox, Oct4, IK, BK, TGF-beta and TGF-beta receptor and MMP2 mRNA (**Figure 7, Figure 8** B-L).

The transfilter co-culture shows significant upregulation of SDF-1 mRNA (**Figure 8** I), whereas this effect cannot be seen in the direct co-culture, thus reflecting the protein immunofluorescence data. In both co-culture techniques U87MG glioblastoma exhibited a, yet not significant, tendency towards higher CXCR4 mRNA abundance as compared to the respective monocultures (**Figure 7, Figure 8** D and I). In combination, those findings hint to an upregulation of the SDF-1/CXCR4 chemokine pathway.

mRNA of the ion channel TRPM8 shows to be significantly reduced through direct co-culture (**Figure 7**C), whereas this effect cannot be seen in a transfilter co-culture (**Figure 8**H). The matrix metalloprotease MMP9 is significantly upregulated through endothelial co-culture suggesting induced invasive potential (**Figure 8**L).

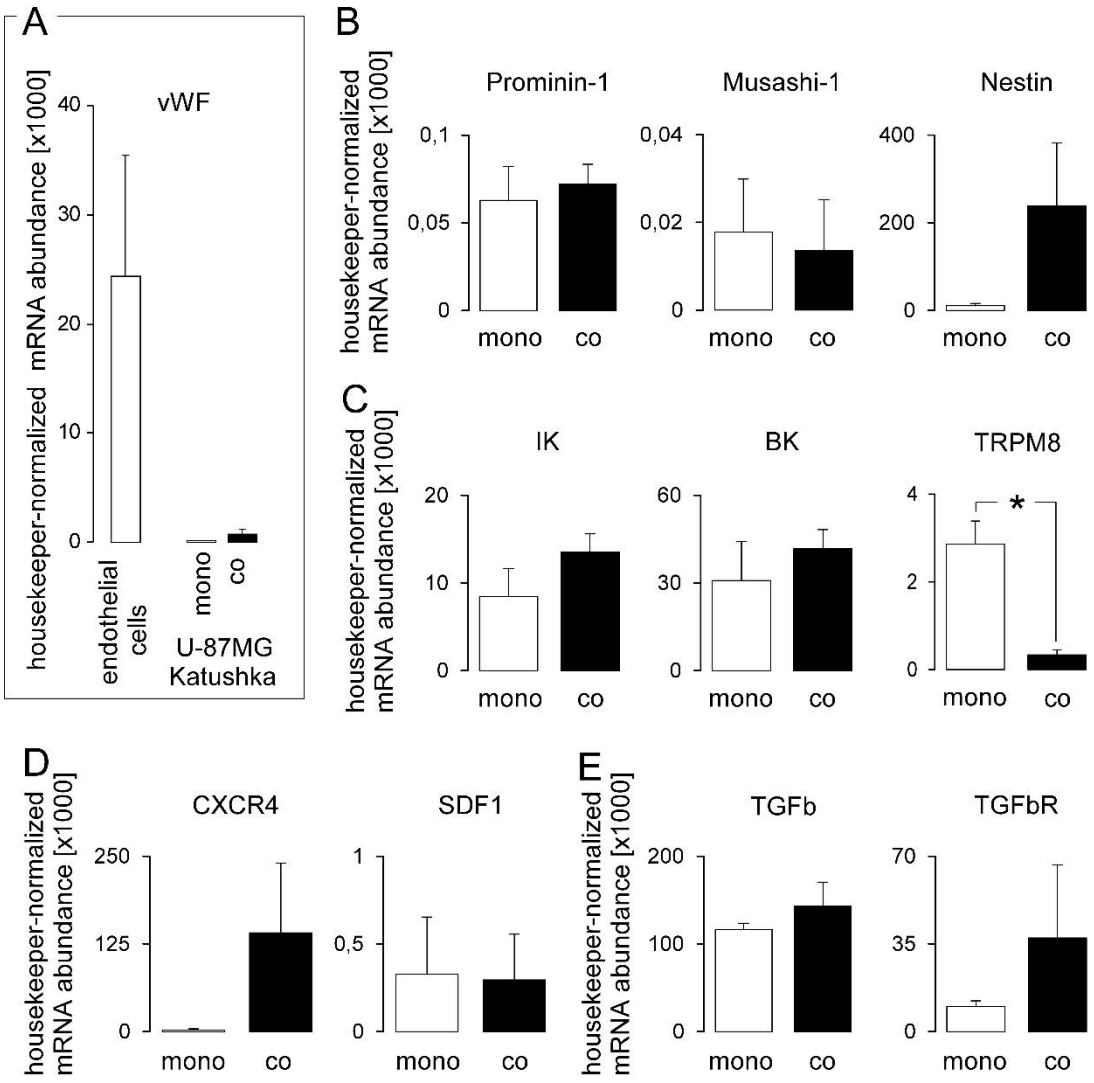

Figure 7. Directly co-cultured endothelial cells (hCMEC/D3) lower mRNA abundance of the ion channel TRPM8 in U87MG-Katushka glioblastoma cells. **A.** Houskeeper-normalized mRNA abundances of the endothelial cell marker Von-Willebrand-factor (vWF) in endothelia cell monocultures (1st bar), in U-87MG-Katushka grown in monocultures (2nd bar) and direct co-cultures with endothelial cells (3rd bar). **B-E**. Houskeeper-normalized abundances of mRNAs encoding for stem cell markers (B), ion channels (C), chemokine signaling (D), and TGF-beta signaling (E). Mean data (± SE, n = 3-4) of U-87MG Katushka cells grown in monoculture (open bars) and co-culture (closed bars) with endothelial cells are shown. Irradiated and non-irradiate samples pooled. * indicate $p \leq 0.05$, two-tailed Welch corrected *t*-test.

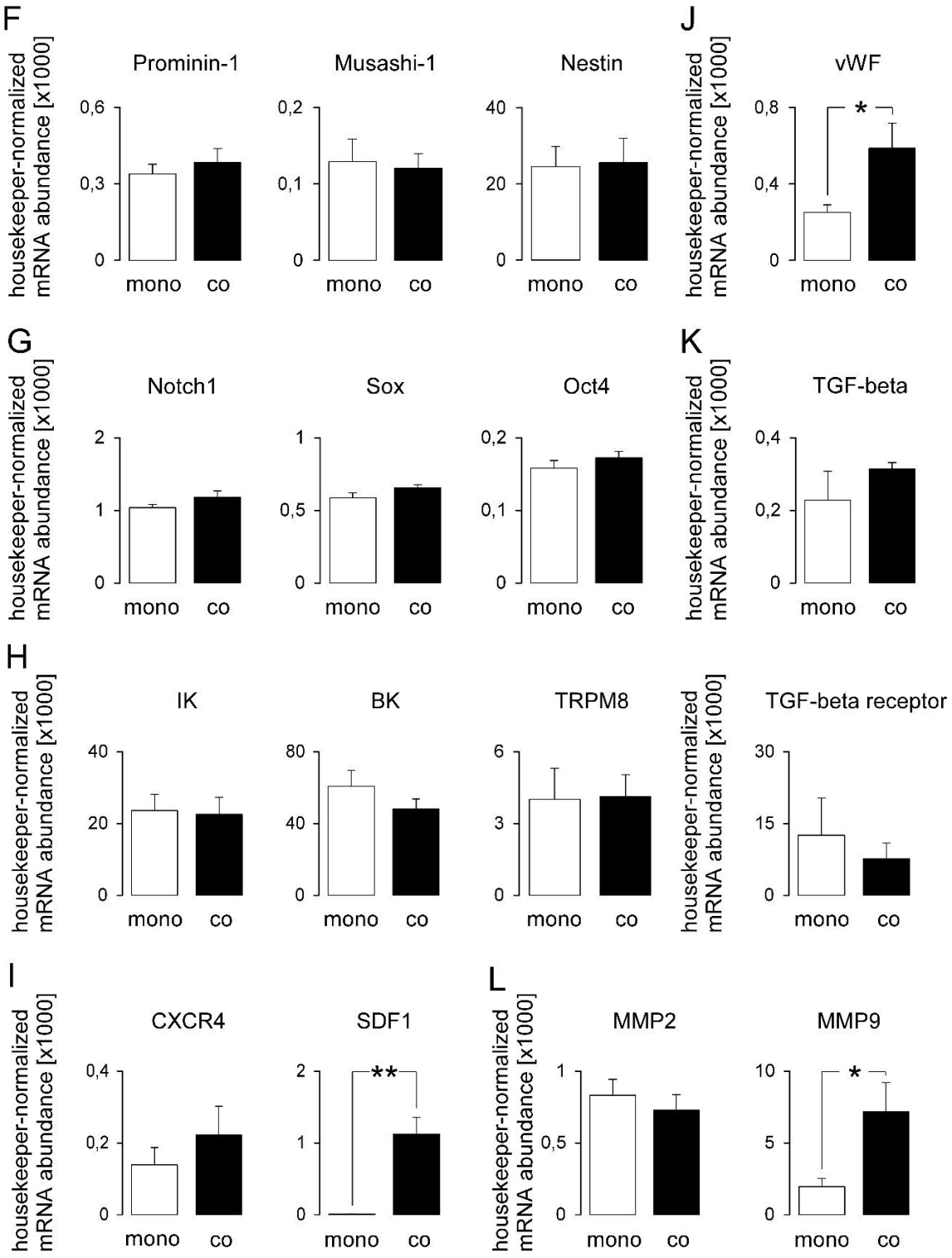

Figure 8. Transfilter co-cultured endothelial cells (hCMEC/D3) induce upregulation of mRNAs involved in cell migration and invasion in U87MG-Katushka glioblastoma cells. **F-L**. Houskeeper-normalized abundances of mRNAs encoding for stem cell markers (F+G), ion channels (H), chemokine signaling (I), endothelial von-Willebrand factor (J), TGF-beta signaling (K), and matrix metalloproteinase (I). Mean data (± SE, n = 4-10) of U-87MG-Katushka cells grown in monoculture (open bars) and filter-separated co-culture (closed bar) with endothelial cells are shown. Irradiated and non-irradiate samples pooled. * and ** indicate $p \leq 0.05$ and $p \leq 0.01$, respectively, two-tailed Welch corrected t-test.

3.2.4 Patch-clamp recording

SDF-1-axis has been reported to stimulate migration through Ca^{2+}-activated, K^{+}-selective ion channels in glioblastoma cells[55]. To test for endothelial cell-induced stimulation of involved ion channel activity, macroscopic on-cell (cell-attached) currents of U-87MG-Katushka cells grown in direct endothelial cell (hCMEC/D3) co-culture (24 – 48 h co-culture time) or monoculture were recorded with the patch-clamp technique in on-cell (cell-attached) voltage-clamp mode (**Figure 9** A). Endothelial cell co-culture stimulated an outward current in U-87MG-Katushka cells at positive voltages (**Figure 9** B-C) which was due to a significant higher conductance (**Figure 9** D) and a shift of the macroscopic current reversal potential by +10 mV (**Figure 9** E).

The on-cell currents at reversal potential and at more negative voltages are mainly due to unbiological leak currents that reverse at 0 mV membrane voltage. So more negative the physiological membrane potential (which applies in on-cell mode together with the clamp voltage to the sealed membrane) so higher must be the clamp voltage to zero the membrane voltage. A shift of the reversal potential towards more positive voltages, therefore, hints to a hyperpolarization of the physiological membrane potential at the sealed membrane patch.

To identify the ion channel type underlying the endothelial cell-induced currents, unitary current transitions of on-cell recording tracings were analyzed (**Figure 10** A). The channel amplitude/voltage relationships (**Figure 10** B) of channels recorded under mono- and co-culturing conditions exhibited a high unitary conductance in the range of 160 pS (**Figure 10** C) and an extrapolated reversal potential which is about -30 mV more negative than the physiological membrane potential (0 mV clamp voltage, Fig. 5D) suggesting a high conductance K+-selective channel. Moreover, the open probability (nPo)/voltage relationship (Fig. 5D) indicates a voltage-dependent activity of the channels. nPo differed markedly between mono- (**Figure 10** D, blue line) and co-cultured (**Figure 10** D, red line) U-87MG-Katushka cells in that way that channel activity was apparent already at 0 mV clamp voltage (i.e., at physiological membrane potential) in co-

cultured glioblastoma cells while monocultures showed channel activity only at higher clamp voltages (**Figure 10** E).

Permselectivity, unitary conductance and voltage-dependence resemble the properties of BK Ca2+-activated K+ channels which have been reported to be highly expressed in glioblastoma cells. Channel activity at physiological membrane potential, i.e., at 0 mV clamp voltage, as observed in U-87MG-Katushka cells grown in co-culture with endothelial cells, however, suggests physiological significance of the channel.

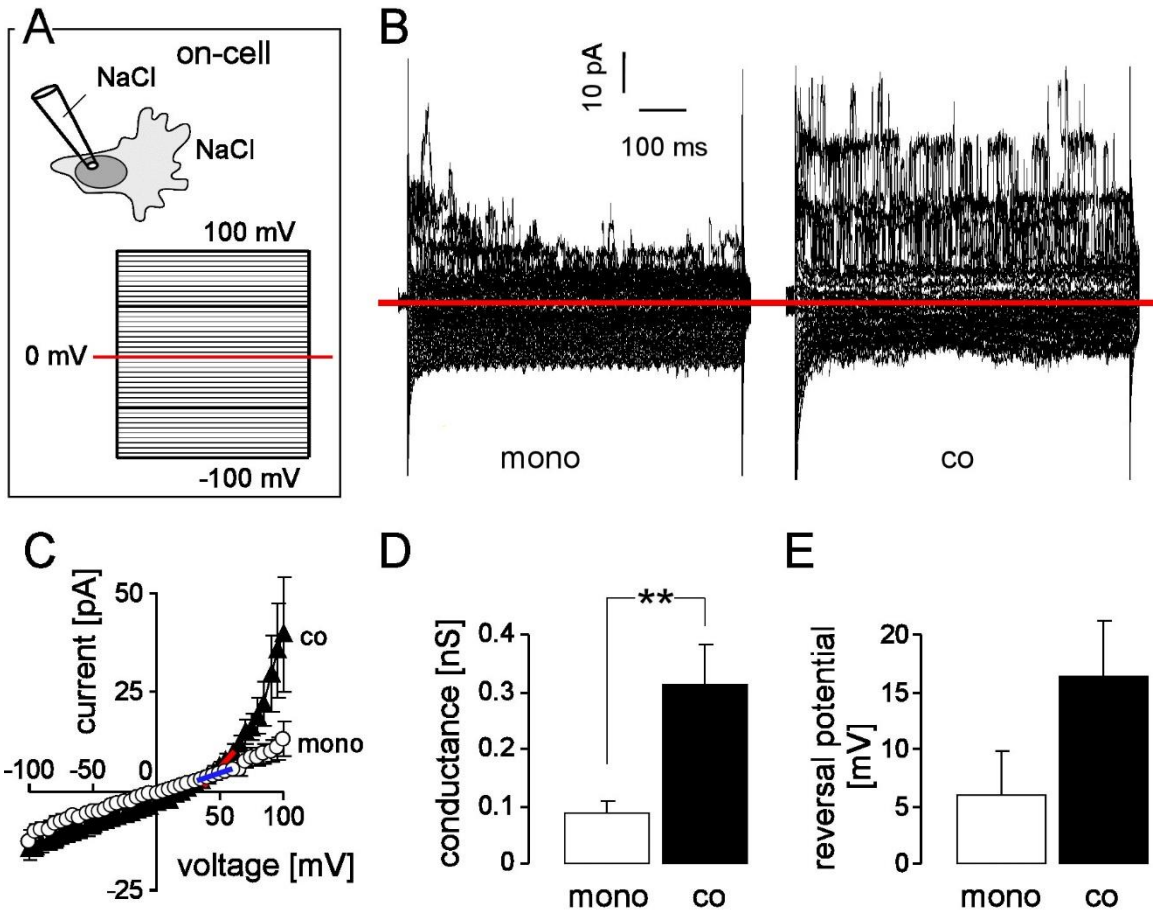

Figure 9. Endothelial cells (hCMEC/D3) induce activation of outward currents in U-87MG-Katushka glioblastoma cells. **A**. Schemes, depicting the pipette and bath solution (top) and the voltage pulse protocol (bottom) applied in on-cell (cell-attached) patch clamp experiments. **B**. Representative on-cell current tracings recorded with the protocol illustrated in (A) in U-87MG-Katushka cells grown in monoculture (left) or direct co-culture with endothelial cells (right). Zero current is indicated by red line, macroscopic current tracings of the individual current sweeps recorded at the different clamp-voltages are superimposed. **C**. Relationship between mean (± SE, n = 9-11 cells) macroscopic on-cell currents and voltage recorded as in (A, B) in U-87MG-Katushka cells grown in monoculture (open circles) or direct co-culture with endothelial cells (closed triangles). **D, E**. Mean (± SE) conductance (D) and reversal potential (E) of the macroscopic on-cell current in U-87MG-Katushka cells grown in monoculture (open bars) or direct co-culture with endothelial cells (closed bars). Data from (C), conductances were calculated by linear regression between +35 mV and + 60 mV (as indicated in (C) by blue and red line). ** indicates $p \leq 0.01$, two-tailed (Welch corrected) t-test.

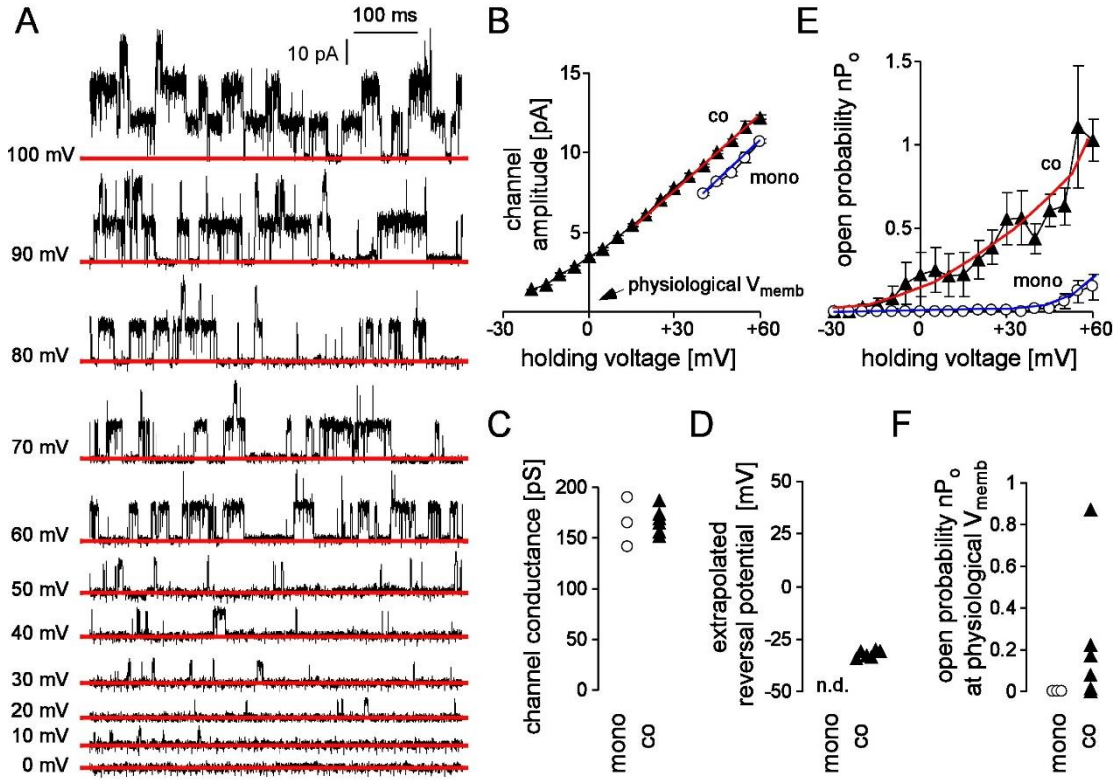

Figure 10. Large conductance, voltage-dependent K+-selective channels generate the outward current induced by endothelial cell (hCMEC/D3) in U-87MG-Katushka cells. **A**. Current tracings of U-87MG-Katushka cells directly co-cultured with endothelial cells recorded at different holding potentials (as indicated) in on-cell mode with NaCl in bath and pipette solutions. **B, E**. Relationship between mean (± SE, n = 3-6) channel amplitude (B) or open probability (nPo, E) and holding potential recorded in U-87MG-Katushka cells grown in monoculture (open circles) or direct co-culture with endothelial cells (closed triangles). **C, D, F**. Conductance (C), reversal potential (D), and open probability (F) of channels recorded in mono- (open circles) and co-cultured U-87MG-Katushka cells (closed triangles). Individual recordings are shown. Conductances in (C) and open probabilities in (F) were given for positive holding potentials (as indicated by red and blue line in (B)) and physiological membrane potential (i.e., 0 mV holding potential), respectively. n. d.: not determinable.

3.2.5 Migration assay

Programming and execution of cell migration is a reported function of BK channels in glioblastoma [55]. Although raises of the BK channels mRNA through endothelial co-culture could not be found, a higher activity in terms of open probability could be shown in the present endothelial-glioblastoma co-culture model, as described before. To test migration and invasive potential on a functional level, transfilter chemotaxis of U-87MG Katushka cells grown in filter separated co-cultures (hCMEC/D3 endothelial cells, 48 – 96 h co-culture time) and in monocultures was quantified in impedance measurements using the Roche xCELLigence system. As a result, co-culturing stimulated transfilter chemotaxis (**Figure 11**), complementing the elevated MMP9 mRNA level as an effector molecule for invasion (see 3.2.2).

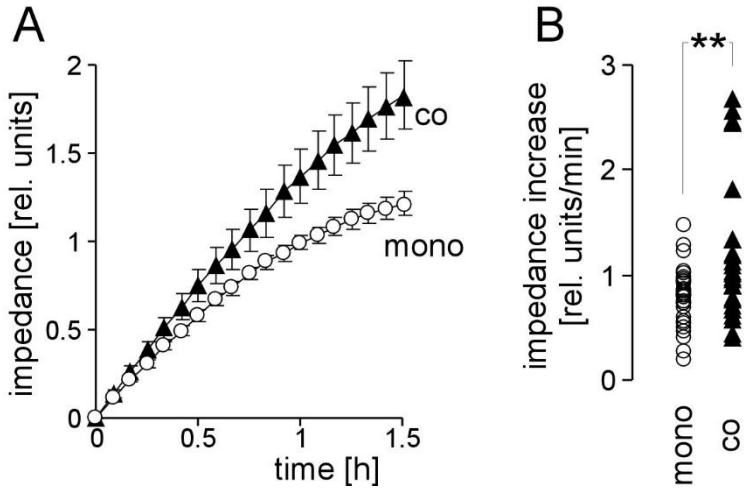

Figure 11. Endothelial cells stimulate transfilter chemotaxis of U-87MG-Katushka cells. **A**. Time course of changes in mean (± SE, n = 28-29) impedance as a real time measure of transfilter chemotaxis (1%/5% FCS gradient) as recorded with the Roche xCelligence Sytem in U87MG-Katushka cells grown in monoculture (open circles) or filter-separated co-culture with endothelial cells (closed triangles). **B**. Transfilter chemotaxis-dependent impedance increase as defined by the slope of the impedance/time relationship between 0 and 1.5 h of monocultured (open circles) and co-cultured U87MG-Katushka cells. Shown are individual experiments, data from (A). ** indicates $p \leq 0.01$, Welch-corrected t-test.

4 Discussion

4.1 Summary of results

As a starting point the SDF-1/CXCR4 axis, a reported pathway of endothelial cell/glioblastoma interaction [62], was analyzed by immunofluorescence of SDF-1. Unexpectedly endothelial co-culture seemed to induce no change in SDF-1 expression. Focus was then shifted to a functional level, examining the influence of endothelial co-culture on radiation induced cell death, radioresistance and clonogenic survival of glioblastoma cells by flow cytometry and colony formation assays. No protecting or self-renewal inducing effect, both indirect markers of stemness, could be observed. After those unexpected findings the human umbilical vein endothelial cells were replaced with human cerebral microvascular endothelial cells to achieve a closer resemblance of the physiological microenvironment. Observation started on a functional level again by quantifying the rate of apoptotic cells in co-cultured glioblastoma cells as an indicator of radioresistance. No radioprotective effect of endothelial co-culturing could be found. To get a more comprehensive view on possible glioblastoma-endothelial cell interactions, the effect of endothelial cell co-culture on mRNA abundances of glioblastoma cells was determined. In particular mRNAs encoding stem cell markers, effector proteins of invasion, cell-signalling-pathways and ion channels, reported to contribute in those interactions, were analyzed. The results suggest endothelial induced changes in in the expression of the TRPM8 ion channel genes, mixed results on the changes in SDF-1 expression and an upregulation of the matrix-metalloproteinase 9 as an effector protein of invasion. The following electrophysiological experiments showed higher open-probability of a voltage dependent K^+-selective ion channels at physiological membrane potential, identified as BK channel. Programming and execution of migration is a reported function of the BK K^+ channel in glioblastoma. A significant endothelial induced induction of transfilter chemotaxis

of glioblastoma cells resemble these electrophysiological findings and the elevated mRNA level of MMP9.

4.2 Addressing the research questions

The present work aimed to examine the effect of an *in vitro* co-culture model of endothelial cells and glioblastoma cells on stem cell properties of the glioblastoma cells, in the form of expression of stem cell markers, clonogenic survival, radioresistance and migration potential.

The first question to be addressed regarding stem cell properties was whether co-culturing with endothelial cells would lead to an upregulation of stem cell markers in glioblastoma cells. This was tested through a polymerase chain reaction of mRNA of the markers.

Although a variety of established stem cell markers, including CD-133, Sox2, Nestin, Notch, Musashi-1, and Oct4, were tested no significant upregulation of those markers could be found in the glioblastoma cells co-cultured with endothelial cells in our model. For some there is *in vitro* endothelial-co-culture data of available.

Two studies have been identified that analysed the effect of endothelial co-culture on CD-133 levels in glioblastoma cells. Fessler et al. showed an increase of the CD-133 positive fraction of glioblastoma cells measured through flow cytometry, after being treated with endothelial-cell-conditioned medium for 24 h[51]. Yan et al. showed a similar increase of CD-133 positive glioblastoma cells in a flow cytometry experiment when co-cultured in a transfilter approach with either mouse brain endothel and HUVECs[48]. While these data seemingly conflict on the first sight, it needs to be mentioned that a rise in the $CD\text{-}133^{+}$ cell fraction must not necessarily be caused by an elevated mRNA level of CD-133, that we could not observe. Downstream processes like a higher transcription rate or increased membrane translocation could be possible explanations for Fessler's and Yan's findings. Further investigation needs to clarify on what

biological level endothelial co-culture influences CD-133 expression. Technically Fessler's use of conditioned medium instead of *in vitro* co-culture is a major difference impeding comparability. By using a direct co-culture, the experimental setting of Yan et al. is more similar to ours but features important differences, too. First, they did not use beta-FGF in their media. It was used in this present work to maintain a stable endothelial differentiation but could inhibit the transformation to a stem-cell-like phenotype of the glioblastoma cells in the same function. Second, mouse derived endothelial and glioma cells were used by Yan et al.. This cell lines may have a different pathology than human cell lines. Our use of the human derived HUVEC and hCMEC might lead to a more reliable co-culture model compared to the use of mouse cell lines.

This is supported by other findings of Yan et al. regarding the stem cell marker Sox2. Sox2 is a transcription factor crucially involved in embryogenesis. While its overexpression is a reported stem cell marker in many malignancies[63, 64], its role as a glioblastoma stem cell marker remains controversial due to universally high expression in differentiated and stem cells and limited prognostic implications[65-67]. Nevertheless, knock-down experiments implicate an effect on tumorigenicity and an important role in glioblastoma cells plasticity between the differentiated and the stem cell state[65, 68]. Yan et al. found an upregulation of Sox2 mRNA in glioblastoma cells through endothelial co-culture in their mouse-endothel/mouse-glioma model. This upregulation was severely reduced in a human-endothel/human-glioblastoma model by Yan et al.. This is congruent with our results regarding Sox2. Unfortunately, Yan et al. do not provide RNA data for CD-133 for comparison with our data.

Chonan et al. co-cultured HUVECs with a "syngeneic…glioblastoma-like tumour" cell line in a 3D co-culture model[69]. Falling in line with our observation, they did not find upregulation of the Nestin mRNA in the co-cultured glioblastoma-like cells. Clearly, the questionable similarity of the used glioblastoma-like cells with patient derived glioblastoma cell lines is the biggest limitation of this study when comparing it with our findings.

The Notch receptor is an exception to the markers mentioned before. Apart from being a stem cell marker itself, the activation of the Notch receptor through its ligand Delta or Jagged, secreted by endothelial cells, is reported to induce stem cell properties in glioblastoma cells[52, 70]. An upregulation of the NOTCH receptor, that could not be shown in our experiments, might have been a hint for activation of the pathway with the result of stem cell formation or maintenance. Oct4 is a transcription factor known for its crucial role in embryogenesis and has then been described as a cancer stem cell marker for various solid tumours [71, 72]. Its role as a cancer stem cell marker for glioblastoma is underlaid by its correlation with poor prognosis in glioblastoma patients, its promotion of clonogenicity of glioblastoma cells and co-expression with other stem cell markers [73-75]. No comparable data regarding Notch and Oct4 for an effect of endothelial co-culture could be found in the literature research.

Altogether, our endothelial cell co-culture model failed to show the hypothesized upregulation of stem cell marker expression. This can be due to the insufficiency of our co-culture model to resemble the physiological organization of the perivascular niche that is necessary for the transition to a stem-cell-like phenotype. This is further addressed in 4.3.

As a preliminary test for clonogenic survival the effect of endothelial co-culture on cell death of glioblastoma cells was investigated. The expected induction of apoptosis through radiation could be observed, as a validation of the method, but no effect of endothelial co-culturing on apoptosis induction of the glioblastoma cells could be shown. This was consistent for the use of Annexin V and caspase activation as independent indicators of apoptosis. As a possible conflict worth of discussion Galan-Moya et al. showed that endothelial-cell-conditioned medium lowered the percentage of apoptotic glioblastoma cells (Annexin V and propidium iodide) compared to a control medium [76]. Comparability to the present work is impaired by the fact that only preselected glioblastoma stem cells (by neurosphere growth, Sox2 and Nestin expression)

were used by Galan-Moya. In addition, the conditioning media differed in its composition besides being exposed to endothelial cells.

A general limitation of flow-cytometry-assessed apoptosis rate is that it categorizes a dynamic process, such as apoptosis, at one single point in time. Performed too early cells undergoing apoptosis later will be missed, performed too late cells already in the state of autophagy can't be registered as apoptotic.

Clonogenic survival itself was assessed through colony formation assays. Clonogenicity is a marker for tumour initiation, a key feature of the postulated glioblastoma stem cells. Here, the number of colonies per plated glioblastoma cells was counted after co-culturing with endothelial cells or monoculture. With two different co-culture combinations (T98g glioblastoma cells with HUVEC and U87MG Katushka with hCMEC) we could not find a significant rise in clonogenicity through endothelial co-culture and therefore no evidence for increased tumour initiation capability.

Two studies were identified that, in parts, examined the influence of endothelial cells on clonogenicity. The work of Fessler et al., mentioned before, showed a rise in clonogenicity of CD-133 negative glioblastoma cells through medium conditioned by endothelial cells[51]. Zhu et al. show an increased clonogenicity of glioblastoma derived neurospheres after directly co-culturing them with brain endothelial cells[52]. While these results undoubtfully conflict with our observations a more detailed view displays important differences in the studies designs. Both studies used preselected cell cohorts. By using only neurosphere cultures (Zhu et al.) the endothelial benefit on clonogenicity can only be proven for cells already identified to carry enriched stem cell features[77]. In contrast Fessler et al. solely used previously isolated CD-133 negative glioblastoma cells. It is not mentioned if the conditioned medium has had a similar effect on CD-133+ cells, but assuming it is not, our unfiltered glioblastoma cell population would have needed a much higher endothelial benefit to show a similar significant increase in clonogenicity.

Moreover, the exposure to the endothelial interaction took place at a different period of the colony formation assay, compared to ours. Fessler et al. used the

conditioned medium during the colony formation period. In an effort to create maximum equality of treatment of the two arms for our experiments, glioblastoma cells were first grown in endothelial co-culture or monoculture and then plated under similar conditions, including the same medium.

As an additional remark, Zhu et al. were using serum free medium, containing FGF and EGF, while Fessler et al. were using none of these components. In our colony formation assay all three components were used during the co-culture period, as a necessity of stable endothelial differentiation, and only FCS used in the colony formation period. The single influence of each of these variables on clonogenicity can't be stated without further experiments.

As stated before, irradiation is one of the main treatment modalities of glioblastoma, especially in recurrent disease. But with glioblastoma having a high inherent level of radioresistance [78], this is mainly due to a lack of efficient alternatives. Additionally, glioblastoma stem cells are reported to even extend the level of radioresistance, partly through their interaction with their microenvironment in the tumour niche.[34, 37, 79]. The colony formation assay with increasing irradiation doses is seen as the gold standard to analyse clinically relevant radiosensitivity [37]. To determine the effect of co-culturing with endothelial cells on clonogenicity under increasing irradiation doses, two combinations of glioblastoma cells and endothelial cells were used (T98g glioblastoma cells with HUVEC and U87MG Katushka with hCMEC). The resulting data showed a shoulder-like decrease of the survival fraction with increasing dosage, as expected, but no difference for glioblastoma cells grown in co-culture or monoculture could be found, in both co-culture combinations. In the absence of comparable literature data, it can be concluded that our co-culture model gives no evidence for increased radioresistance of glioblastoma cells through glioblastoma-endothelial interaction.

Migration and invasion are key features of the pathology of glioblastoma. The cytokine SDF-1 and its receptor CXCR4 form an axis known for mediating chemotaxis and migration[80, 81]. This has been shown especially for gliomas among other malignancies[82]. Hereby SDF-1 is secreted by endothelial cells[62] and modifies critical pathological properties of glioblastoma cells[83].

To investigate the role of this chemokine axis in a glioblastoma-endothelial-cell co-culture model we examined the abundance of SDF-1 and its receptor CXCR4 in glioblastoma cells growing in endothelial-cell co-culture and monoculture on the mRNA level. The significant upregulation of SDF-1 in the transfilter co-culture is congruent with similar findings of Yan et al [48], whereas they do not report about the receptor CXCR4, for which a yet not significant tendency towards upregulation could be shown.

The contrasting unaltered SDF-1 mRNA levels in the direct co-culture have then been paralleled by immunofluorescence experiments showing no significant differences in SDF-1 expression of glioblastoma cells (U87MG Katushka) growing in endothelial co-culture and those who did not. To solve this dissent further experiments are needed. However, the basis of this reflection could be confirmed by showing a significant high abundance of SDF-1 inside the endothelial cells.

Another cytokine reported to be playing a role in glioblastoma migration [84, 85], TGF-β and its receptor TGF-β-R didn’t show altered levels of mRNA in glioblastoma cells co-cultured with endothelial cells.

SDF-1 has been shown to stimulate glioblastoma migration, partly through the activation of the BK K^+-channel [55, 82]. Despite the fact, that we could not show changes in mRNA abundance of the ion channels BK, IK through endothelial co-culture, we could prove a significant rise of the open probability of a K^+-selective ion channel identified as BK in on-cell patch-clamp measurements. This gain of the BK-channel activity without a rise of mRNA abundance through endothelial co-culture may be due to downstream changes of the cellular BK-channel formation after translation to mRNA. More contradictory is the role of the ion channel TRPM8. It is reported to be highly upregulated in glioblastoma and has

been shown to be a driver of migration and radioresistance *in vitro* [86, 87]. Given this, interpreting our finding of significantly reduced TRPM8 expression in glioblastoma through direct endothelial co-culture could suggest an inhibitory effect on migration potential. However, a small retrospective analysis found a correlation between high TRPM8 levels and a more favourable prognosis [88].

As an endpoint of this part of the research question functional migration of glioblastoma cells was studied in an *in vitro* quantitative cell migration assay. In concordance to the elevated BK-channel activity glioblastoma cells of the U87MG Katushka cell line co-cultured with endothelial cells showed a significantly stimulated transmembrane chemotaxis in comparison to those previously grown in monoculture.

Another finding worth to be addressed in the context of migration is the described elevation of the abundance of MMP-9 in glioblastoma cells, co-cultured with endothelial cells. Although this protease of the extracellular matrix is not directly linked with migration, it has been studied intensively as an effector molecule for invasion[89, 90]. Certainly, these two processes necessitate each other in an *in vivo* environment. The shown upregulation of MMP-9 in glioblastoma cells through endothelial co-culture is also verifying the data of Kenig at al.[62].

Summarized, our experiments imply BK-channel activity mediated increase of the migration potential of glioblastoma cells, when grown in endothelial co-culture. This process seems to be driven by endothelial secretion of SDF-1 and possible juxtacrine autostimulation with SDF-1 of the glioblastoma cells and is paralleled by an elevated invasive potential of those.

4.3 Co-culture model

In the present work the interaction between endothelial cells and glioblastoma cells was studied using a direct co-culture environment of both cell types and a transfilter co-culture with an endothelial monolayer on the downward-facing filter

membrane face and 3µm pores. Both techniques allow paracrine and direct cell-to-cell communication. Co-culture time was in a range from 24-96 hours allowing metabolic changes on multiple levels including RNA and protein expression.

Despite these features this technique faces multiple limitations compared to the physiological situation. Two-dimensional culture surfaces, as have been used, cannot mirror the three-dimensional reality, where e.g. a much higher density of direct cell-to-cell and juxtacrine communication is possible or the concentration of paracrine transmitters could presumably reach much higher levels. Another possible constraint is the need to change the cell culture medium or ad fresh medium to ensure nutrition supply and pH regulation. This possibly dilutes or washes out those transmitters.

Given, that the co-culture time was suitable for short term metabolic changes, by the time of coculturing the glioblastoma cell lines consisted of differentiated cancer cells. Conceivably crucial endothelial-glioblastoma interactions may take place during cancerogenesis, which would be missed in the given co-culture model. Furthermore, medium supplements necessary for the maintenance of the endothelial differentiation may mask or suppress metabolic changes in the glioblastoma cells. Possible targets of this assumption are e.g. the concentration of bovine serum and the addition of beta-FGF to the culture medium. There is evidence for both substances to influence stemness[91, 92] for the one and endothelial-glioblastoma- communication[51] for the latter. These limitations may have had significant effects on the tested parameters, masking the physiological processes.

Nonetheless, endothelial cells are only one yet important factor of the glioblastoma tumour or stem cell niche. Possible interactions in the niche have been reported for pericytes, microglia and extra-cellular-matrix components [37, 93] Their integration would require more advanced *in vitro* models of the glioblastoma microenvironment in order to fully comprehend glioblastoma physiology.

4.4 Conclusion and further perspective

The work at hand tries to elucidate the role of endothelial cells in glioblastoma perivascular stem cell niches in an *in vitro* study. Taken together, these data provide evidence for an interaction between endothelial cells and glioblastoma cells. Endothelial cells stimulate migration potential in the form of chemotaxis and probably also invasion. This stimulation seems to be induced by endothelial- and auto-secreted SDF-1 and mediated by increased BK K+ channel activity. In our co-culture model, no effect of endothelial cells on upregulation of stem cell markers, clonogenicity or radioresistance of the glioblastoma cells was observed. Despite the described limitations of this study, the presented data contribute to understanding the pathophysiology of glioblastoma stem-like cells in their niche. Further research in this field should aim to develop more advanced models of the tumour microenvironment. This could include a three-dimensional co-culture model to mimic migration and invasion processes. In addition, the roles of other cell types such as astrocytes and microglia should be investigated. Although this is foundational research our common aim is to find new treatment approaches. Derived from this work the inhibition of SDF-1 stimulated and BK-channel mediated migration of glioblastoma, could be a pharmacologic approach to improve treatment and prognosis of our patients.

5 Summary

Glioblastoma (GB) is the most frequent malignant primary brain tumour in adults. Despite multimodal therapy prognosis of this locally invasive tumour remains poor. The adaption of the cancer stem cell hypothesis has resulted in a postulated glioblastoma stem cell (GCS) population. This subpopulation is characterized by extended capabilities of self-renewal, tumour initiation and therapy resistance. GCS are located in close proximity to tumour vessels. This special microenvironment of GCS has been defined as perivascular stem cell niche. Endothelial co-culture of glioblastoma cells has been shown to enrich the GCS population in *in vitro* experiments. The present medical doctoral thesis seeks to establish an *in vitro* GB/endothelial co-culture model to analyze the effect of endothelial co-culture on stem cell properties of GB cells. Upregulation of stem cell markers, clonogenic survival, radioresistance and migration potential were tested. Therefore, two GB cell-lines (U87MG Katushka, T98G) were co-cultured with two different human endothelial cell-lines (HUVEC, hCMEC/D3) in direct and transfilter co-culture techniques. Radioresistance and clonogenic survival were investigated by flow cytometry and colony formation assays. Migration potential was analyzed through immunofluorescence and RT-PCR of its signalling pathway molecules SDF1/CXCR4, patch-clamp recording of its effector ion channels and on a functional level by *in vitro* real-time migration assays. Expression of stem cell markers, corresponding ion channels and effector molecules of invasive potential was analyzed with RT-PCR. In the established *in vitro* co-culture model, endothelial cells stimulate migration, illustrated by significantly increased chemotaxis of GB cells. This stimulation might be induced by observed endothelial- and auto-secreted SDF-1 and mediated by increased BK K^+ channel activity. In addition, co-cultured GB cells show a significant upregulation of matrix metalloproteinases, indicating increased invasive potential. In this co-culture model, no effect on stem cell markers, clonogenicity or radioresistance of the GB cells, derived from colony formation assays and flow cytometry, was observed. The increased *in vitro* migration potential of GB cells by endothelial co-culture is presented for the first time. Our data are congruent with recent literature regarding elevated matrix

metalloproteinases levels, increased SDF-1 expression and unaltered levels of most stem cell markers. In contrast, upregulation of stem cell markers, as well as increased clonogenic survival of GB cells through endothelial co-culture or conditioned medium reported by other groups could not be reproduced in the present experiments, given significant differences in the experimental setting. Considering the inherent limitations of an in vitro, two-dimensional co-culture model, the presented data provide evidence for an interaction between endothelial cells and glioblastoma cells in the form of stimulated migration and probably also invasion and therefore contribute to the understanding of the perivascular stem cell niches. This may provide target structures for new treatment approaches for GB.

6 Zusammenfassung

Das Glioblastoma multiforme (GB) ist der häufigste bösartige Hirntumor des Erwachsenen. Trotz multimodaler Therapie ist die Prognose dieses lokalinvasiven Tumors schlecht. Die Adaption der Krebsstammzellhypothese führte zur Postulierung einer Stammzellsubpopulation in Glioblastomen (GCS). Diese ist durch die Fähigkeit zur Selbsterneuerung, Tumorinitiierung und Therapieresistenz charakterisiert. GCS finden sich vorwiegend in räumlicher Nähe der Tumorvaskularisierung. Dieses spezielle Mikromilieu wird als perivaskuläre Stammzellnische bezeichnet. Eine Kokultivierung von Endothel- und Glioblastomzellen zeigte darüber hinaus eine Vermehrung der GCS Fraktion in *in vitro* Experimenten. In der vorliegenden Dissertation wurden die Effekte eines *in vitro* GBM/Endothel-Kokulturmodells auf die Stammzelleigenschaften von Glioblastomzellen in Form von Stammzellmarkern, klonogenem Überleben, Radioresistenz und Migrationspotential untersucht. Hierfür wurden zwei humane Glioblastomzellreihen (U87MG Katushka, T98G) mit zwei humanen Endothelzellreihen (HUVEC, hCMEC/D3) in direkter und transfilter Technik kokultiviert. Radioresistenz und klonogenes Überleben wurden mittels Durchflusszytometrie und Koloniebildungstest untersucht. Das Migrationspotential wurde durch Immunfluoreszenz und RT-PCR des SDF-1/CXCR4 Signalweges, Patch-Clamp-Messungen des Effektor-Ionenkanals sowie durch einen funktionellen *in vitro* real-time Migrationsassay analysiert. Die Expression von Stammzellmarkern, korrespondierender Signalmoleküle und Ionenkanälen, sowie von Invasionsproteinen wurde mittels RT-PCR getestet. In dem gezeigten *in vitro* Kokulturmodell stimulieren Endothelzellen das Migrationspotential von Glioblastomzellen im Sinne einer signifikant gesteigerten Chemotaxis. Diese Stimulation scheint durch eine hierbei beobachtete endotheliale sowie Auto-Sekretion von SDF-1 induziert und durch eine erhöhte BK K^+ Kanalaktivität vermittelt zu sein. Zusätzlich impliziert eine signifikant erhöhte Expression von Matrixmetalloproteinasen in kokultivierten Glioblastomzellen ein erhöhtes Invasionspotential. Es konnte kein Effekt auf die Stammzellmarkerexpression, die Klonogenität oder Radioresistenz der kokultivierten Glioblastomzellen beobachtet werden. Das gesteigerte *in vitro*

Migrationspotential durch eine endotheliale Kokultur wird in dieser Arbeit erstmalig beschrieben. Die präsentierten Daten zur Erhöhung der Matrixmetalloproteinasen sowie der erhöhten SDF-1 Expression und unveränderter Level der meisten Stammzellmarker stehen in Einklang mit bisherigen Literaturberichten. Die in anderen Studien berichte erhöhte Klonogenität und Stammzellmarkerexpression durch endotheliale Ko-Kultur oder konditioniertes Medium konnte in dieser Arbeit nicht reproduziert werden. Wobei hier signifikante Unterschiede des experimentellen Aufbaus bestehen. Unter Berücksichtigung der inhärenten Limitationen eines zweidimensionalen *in vitro* Kokulturmodells, liefern die präsentierten Daten Hinweise für eine Interaktion von Endothel und Glioblastomzellen in Form von gesteigertem Migrations und Invasionspotential und tragen damit zum Verständnis der Pathomechanismen der perivaskulären Stammzellnische bei. Diese könnte als mögliche Zielstruktur neuer Therapieansätze des Glioblastoms dienen.

7 Literature

1. Ostrom, Q.T., et al., *The epidemiology of glioma in adults: a "state of the science" review.* Neuro Oncol, 2014. **16**(7): p. 896-913.
2. Tamimi, A.F. and M. Juweid, *Epidemiology and Outcome of Glioblastoma*, in *Glioblastoma*, S. De Vleeschouwer, Editor. 2017: Brisbane (AU).
3. Aldape, K., et al., *Glioblastoma: pathology, molecular mechanisms and markers.* Acta Neuropathol, 2015. **129**(6): p. 829-48.
4. Cuddapah, V.A., et al., *A neurocentric perspective on glioma invasion.* Nat Rev Neurosci, 2014. **15**(7): p. 455-65.
5. Claes, A., A.J. Idema, and P. Wesseling, *Diffuse glioma growth: a guerilla war.* Acta Neuropathol, 2007. **114**(5): p. 443-58.
6. Alcantara Llaguno, S., et al., *Malignant astrocytomas originate from neural stem/progenitor cells in a somatic tumor suppressor mouse model.* Cancer Cell, 2009. **15**(1): p. 45-56.
7. Alcantara Llaguno, S., et al., *Cell-of-origin susceptibility to glioblastoma formation declines with neural lineage restriction.* Nat Neurosci, 2019. **22**(4): p. 545-555.
8. Sanai, N., A. Alvarez-Buylla, and M.S. Berger, *Neural stem cells and the origin of gliomas.* N Engl J Med, 2005. **353**(8): p. 811-22.
9. Louis, D.N., et al., *The 2016 World Health Organization Classification of Tumors of the Central Nervous System: a summary.* Acta Neuropathol, 2016. **131**(6): p. 803-20.
10. Perry, J.R., et al., *Short-Course Radiation plus Temozolomide in Elderly Patients with Glioblastoma.* N Engl J Med, 2017. **376**(11): p. 1027-1037.
11. Stupp, R., et al., *Effects of radiotherapy with concomitant and adjuvant temozolomide versus radiotherapy alone on survival in glioblastoma in a randomised phase III study: 5-year analysis of the EORTC-NCIC trial.* Lancet Oncol, 2009. **10**(5): p. 459-66.
12. Herrlinger, U., et al., *Lomustine-temozolomide combination therapy versus standard temozolomide therapy in patients with newly diagnosed glioblastoma with methylated MGMT promoter (CeTeG/NOA-09): a randomised, open-label, phase 3 trial.* Lancet, 2019. **393**(10172): p. 678-688.
13. Hegi, M.E., et al., *MGMT gene silencing and benefit from temozolomide in glioblastoma.* N Engl J Med, 2005. **352**(10): p. 997-1003.
14. Brandes, A.A., et al., *Recurrence pattern after temozolomide concomitant with and adjuvant to radiotherapy in newly diagnosed patients with glioblastoma: correlation With MGMT promoter methylation status.* J Clin Oncol, 2009. **27**(8): p. 1275-9.
15. Rapp, M., et al., *Recurrence Pattern Analysis of Primary Glioblastoma.* World Neurosurg, 2017. **103**: p. 733-740.
16. Minniti, G., et al., *Patterns of failure and comparison of different target volume delineations in patients with glioblastoma treated with conformal radiotherapy plus concomitant and adjuvant temozolomide.* Radiother Oncol, 2010. **97**(3): p. 377-81.
17. Chen, L., et al., *Glioblastoma recurrence patterns near neural stem cell regions.* Radiother Oncol, 2015. **116**(2): p. 294-300.
18. Clevers, H., *The cancer stem cell: premises, promises and challenges.* Nat Med, 2011. **17**(3): p. 313-9.
19. Bonnet, D. and J.E. Dick, *Human acute myeloid leukemia is organized as a hierarchy that originates from a primitive hematopoietic cell.* Nat Med, 1997. **3**(7): p. 730-7.
20. Matsui, W., et al., *Characterization of clonogenic multiple myeloma cells.* Blood, 2004. **103**(6): p. 2332-6.

21. Lapidot, T., et al., *A cell initiating human acute myeloid leukaemia after transplantation into SCID mice.* Nature, 1994. **367**(6464): p. 645-8.
22. Sin, W.C. and C.L. Lim, *Breast cancer stem cells-from origins to targeted therapy.* Stem Cell Investig, 2017. **4**: p. 96.
23. Feng, L., J.B. Wu, and F.M. Yi, *Isolation and phenotypic characterization of cancer stem-like side population cells in colon cancer.* Mol Med Rep, 2015. **12**(3): p. 3531-6.
24. Hardavella, G., R. George, and T. Sethi, *Lung cancer stem cells-characteristics, phenotype.* Transl Lung Cancer Res, 2016. **5**(3): p. 272-9.
25. Zakaria, N., et al., *Targeting Lung Cancer Stem Cells: Research and Clinical Impacts.* Front Oncol, 2017. **7**: p. 80.
26. Baumann, M., M. Krause, and R. Hill, *Exploring the role of cancer stem cells in radioresistance.* Nat Rev Cancer, 2008. **8**(7): p. 545-54.
27. Schulz, A., et al., *Cancer Stem Cells and Radioresistance: DNA Repair and Beyond.* Cancers (Basel), 2019. **11**(6).
28. Ignatova, T.N., et al., *Human cortical glial tumors contain neural stem-like cells expressing astroglial and neuronal markers in vitro.* Glia, 2002. **39**(3): p. 193-206.
29. Singh, S.K., et al., *Identification of human brain tumour initiating cells.* Nature, 2004. **432**(7015): p. 396-401.
30. Lesueur, P., et al., *Radiosensitization Effect of Talazoparib, a Parp Inhibitor, on Glioblastoma Stem Cells Exposed to Low and High Linear Energy Transfer Radiation.* Sci Rep, 2018. **8**(1): p. 3664.
31. Liu, Y., et al., *Mechanisms regulating radiosensitivity of glioma stem cells.* Neoplasma, 2017. **64**(5): p. 655-665.
32. Liebelt, B.D., et al., *Glioma Stem Cells: Signaling, Microenvironment, and Therapy.* Stem Cells Int, 2016. **2016**: p. 7849890.
33. Chen, J., et al., *A restricted cell population propagates glioblastoma growth after chemotherapy.* Nature, 2012. **488**(7412): p. 522-6.
34. Bao, S., et al., *Glioma stem cells promote radioresistance by preferential activation of the DNA damage response.* Nature, 2006. **444**(7120): p. 756-60.
35. Lomonaco, S.L., et al., *The induction of autophagy by gamma-radiation contributes to the radioresistance of glioma stem cells.* Int J Cancer, 2009. **125**(3): p. 717-22.
36. Wang, J., et al., *Notch promotes radioresistance of glioma stem cells.* Stem Cells, 2010. **28**(1): p. 17-28.
37. Mannino, M. and A.J. Chalmers, *Radioresistance of glioma stem cells: intrinsic characteristic or property of the 'microenvironment-stem cell unit'?* Mol Oncol, 2011. **5**(4): p. 374-86.
38. Chang, C.J., et al., *Enhanced radiosensitivity and radiation-induced apoptosis in glioma CD133-positive cells by knockdown of SirT1 expression.* Biochem Biophys Res Commun, 2009. **380**(2): p. 236-42.
39. Carruthers, R., et al., *Abrogation of radioresistance in glioblastoma stem-like cells by inhibition of ATM kinase.* Mol Oncol, 2015. **9**(1): p. 192-203.
40. Yuan, X., et al., *Isolation of cancer stem cells from adult glioblastoma multiforme.* Oncogene, 2004. **23**(58): p. 9392-400.
41. Brescia, P., et al., *CD133 is essential for glioblastoma stem cell maintenance.* Stem Cells, 2013. **31**(5): p. 857-69.
42. Man, J., et al., *Hypoxic Induction of Vasorin Regulates Notch1 Turnover to Maintain Glioma Stem-like Cells.* Cell Stem Cell, 2018. **22**(1): p. 104-118 e6.
43. Glazer, R.I., D.T. Vo, and L.O. Penalva, *Musashi1: an RBP with versatile functions in normal and cancer stem cells.* Front Biosci (Landmark Ed), 2012. **17**: p. 54-64.

44. Shen, Q., et al., *Endothelial cells stimulate self-renewal and expand neurogenesis of neural stem cells.* Science, 2004. **304**(5675): p. 1338-40.
45. Calabrese, C., et al., *A perivascular niche for brain tumor stem cells.* Cancer Cell, 2007. **11**(1): p. 69-82.
46. Hira, V.V., et al., *CD133+ and Nestin+ Glioma Stem-Like Cells Reside Around CD31+ Arterioles in Niches that Express SDF-1alpha, CXCR4, Osteopontin and Cathepsin K.* J Histochem Cytochem, 2015. **63**(7): p. 481-93.
47. Hira, V.V.V., D.A. Aderetti, and C.J.F. van Noorden, *Glioma Stem Cell Niches in Human Glioblastoma Are Periarteriolar.* J Histochem Cytochem, 2018: p. 22155417752676.
48. Yan, G.N., et al., *Endothelial cells promote stem-like phenotype of glioma cells through activating the Hedgehog pathway.* J Pathol, 2014. **234**(1): p. 11-22.
49. Furnari, F.B., et al., *Malignant astrocytic glioma: genetics, biology, and paths to treatment.* Genes Dev, 2007. **21**(21): p. 2683-710.
50. Sie, M., et al., *Tumour vasculature and angiogenic profile of paediatric pilocytic astrocytoma; is it much different from glioblastoma?* Neuropathol Appl Neurobiol, 2010. **36**(7): p. 636-47.
51. Fessler, E., T. Borovski, and J.P. Medema, *Endothelial cells induce cancer stem cell features in differentiated glioblastoma cells via bFGF.* Mol Cancer, 2015. **14**: p. 157.
52. Zhu, T.S., et al., *Endothelial cells create a stem cell niche in glioblastoma by providing NOTCH ligands that nurture self-renewal of cancer stem-like cells.* Cancer Res, 2011. **71**(18): p. 6061-72.
53. Stein, G.H., *T98G: an anchorage-independent human tumor cell line that exhibits stationary phase G1 arrest in vitro.* J Cell Physiol, 1979. **99**(1): p. 43-54.
54. Allen, M., et al., *Origin of the U87MG glioma cell line: Good news and bad news.* Sci Transl Med, 2016. **8**(354): p. 354re3.
55. Edalat, L., et al., *BK K+ channel blockade inhibits radiation-induced migration/brain infiltration of glioblastoma cells.* Oncotarget, 2016. **7**(12): p. 14259-78.
56. Koopman, G., et al., *Annexin V for flow cytometric detection of phosphatidylserine expression on B cells undergoing apoptosis.* Blood, 1994. **84**(5): p. 1415-20.
57. Vermes, I., et al., *A novel assay for apoptosis. Flow cytometric detection of phosphatidylserine expression on early apoptotic cells using fluorescein labelled Annexin V.* J Immunol Methods, 1995. **184**(1): p. 39-51.
58. Matt Sylte, M.O.B., Thomas Inzana, Chuck Czuprynski, *CaspACE FITC-VAD-FMK In Situ Marker for Apoptosis: Applications for Flow Cytometry.* Promega Notes, 2000. **75**: p. 20–23.
59. Shcherbo, D., et al., *Bright far-red fluorescent protein for whole-body imaging.* Nat Methods, 2007. **4**(9): p. 741-6.
60. Gurskaya, N.G., et al., *GFP-like chromoproteins as a source of far-red fluorescent proteins.* FEBS Lett, 2001. **507**(1): p. 16-20.
61. Hermanson, *Bioconjugate Techniques*. 3rd ed. 2013.
62. Kenig, S., et al., *Glioblastoma and endothelial cells cross-talk, mediated by SDF-1, enhances tumour invasion and endothelial proliferation by increasing expression of cathepsins B, S, and MMP-9.* Cancer Lett, 2010. **289**(1): p. 53-61.
63. Boumahdi, S., et al., *SOX2 controls tumour initiation and cancer stem-cell functions in squamous-cell carcinoma.* Nature, 2014. **511**(7508): p. 246-50.
64. Vanner, R.J., et al., *Quiescent sox2(+) cells drive hierarchical growth and relapse in sonic hedgehog subgroup medulloblastoma.* Cancer Cell, 2014. **26**(1): p. 33-47.
65. Berezovsky, A.D., et al., *Sox2 promotes malignancy in glioblastoma by regulating plasticity and astrocytic differentiation.* Neoplasia, 2014. **16**(3): p. 193-206, 206 e19-25.

66. Phi, J.H., et al., *Sox2 expression in brain tumors: a reflection of the neuroglial differentiation pathway.* Am J Surg Pathol, 2008. **32**(1): p. 103-12.
67. Dahlrot, R.H., et al., *What is the clinical value of cancer stem cell markers in gliomas?* Int J Clin Exp Pathol, 2013. **6**(3): p. 334-48.
68. Gangemi, R.M., et al., *SOX2 silencing in glioblastoma tumor-initiating cells causes stop of proliferation and loss of tumorigenicity.* Stem Cells, 2009. **27**(1): p. 40-8.
69. Chonan, Y., et al., *Endothelium-induced three-dimensional invasion of heterogeneous glioma initiating cells in a microfluidic coculture platform.* Integr Biol (Camb), 2017. **9**(9): p. 762-773.
70. Fan, X., et al., *NOTCH pathway blockade depletes CD133-positive glioblastoma cells and inhibits growth of tumor neurospheres and xenografts.* Stem Cells, 2010. **28**(1): p. 5-16.
71. Kumar, S.M., et al., *Acquired cancer stem cell phenotypes through Oct4-mediated dedifferentiation.* Oncogene, 2012. **31**(47): p. 4898-911.
72. Koo, B.S., et al., *Oct4 is a critical regulator of stemness in head and neck squamous carcinoma cells.* Oncogene, 2015. **34**(18): p. 2317-24.
73. Choi, S.H., et al., *OCT4B Isoform Promotes Anchorage-Independent Growth of Glioblastoma Cells.* Mol Cells, 2019. **42**(2): p. 135-142.
74. Du, Z., et al., *Oct4 is expressed in human gliomas and promotes colony formation in glioma cells.* Glia, 2009. **57**(7): p. 724-33.
75. Guo, Y., et al., *Expression profile of embryonic stem cell-associated genes Oct4, Sox2 and Nanog in human gliomas.* Histopathology, 2011. **59**(4): p. 763-75.
76. Galan-Moya, E.M., et al., *Endothelial secreted factors suppress mitogen deprivation-induced autophagy and apoptosis in glioblastoma stem-like cells.* PLoS One, 2014. **9**(3): p. e93505.
77. Pavon, L.F., et al., *In vitro Analysis of Neurospheres Derived from Glioblastoma Primary Culture: A Novel Methodology Paradigm.* Front Neurol, 2014. **4**: p. 214.
78. Herrmann, T., M. Baumann, and W. Dörr, *Klinische Strahlenbiologie kurz und bündig*. 4., völlig überarb. Aufl. ed. 2006, München Jena: Elsevier Urban & Fischer. VIII, 219 S.
79. Hardee, M.E., et al., *Resistance of glioblastoma-initiating cells to radiation mediated by the tumor microenvironment can be abolished by inhibiting transforming growth factor-beta.* Cancer Res, 2012. **72**(16): p. 4119-29.
80. Dona, E., et al., *Directional tissue migration through a self-generated chemokine gradient.* Nature, 2013. **503**(7475): p. 285-9.
81. Aversa, I., et al., *Epithelial-to-mesenchymal transition in FHC-silenced cells: the role of CXCR4/CXCL12 axis.* J Exp Clin Cancer Res, 2017. **36**(1): p. 104.
82. Sciaccaluga, M., et al., *CXCL12-induced glioblastoma cell migration requires intermediate conductance Ca2+-activated K+ channel activity.* Am J Physiol Cell Physiol, 2010. **299**(1): p. C175-84.
83. Gravina, G.L., et al., *The novel CXCR4 antagonist, PRX177561, reduces tumor cell proliferation and accelerates cancer stem cell differentiation in glioblastoma preclinical models.* Tumour Biol, 2017. **39**(6): p. 1010428317695528.
84. Liu, C.A., et al., *Migration/Invasion of Malignant Gliomas and Implications for Therapeutic Treatment.* Int J Mol Sci, 2018. **19**(4).
85. Li, Q., et al., *MicroRNA-663 inhibits the proliferation, migration and invasion of glioblastoma cells via targeting TGF-beta1.* Oncol Rep, 2016. **35**(2): p. 1125-34.
86. Wondergem, R., et al., *HGF/SF and menthol increase human glioblastoma cell calcium and migration.* Biochem Biophys Res Commun, 2008. **372**(1): p. 210-5.
87. Klumpp, D., et al., *TRPM8 is required for survival and radioresistance of glioblastoma cells.* Oncotarget, 2017. **8**(56): p. 95896-95913.

88. Alptekin, M., et al., *Gene expressions of TRP channels in glioblastoma multiforme and relation with survival.* Tumour Biol, 2015. **36**(12): p. 9209-13.
89. Stamenkovic, I., *Matrix metalloproteinases in tumor invasion and metastasis.* Semin Cancer Biol, 2000. **10**(6): p. 415-33.
90. Rao, J.S., *Molecular mechanisms of glioma invasiveness: the role of proteases.* Nat Rev Cancer, 2003. **3**(7): p. 489-501.
91. Gaelzer, M.M., et al., *Hypoxic and Reoxygenated Microenvironment: Stemness and Differentiation State in Glioblastoma.* Mol Neurobiol, 2017. **54**(8): p. 6261-6272.
92. Behnan, J., et al., *Differential propagation of stroma and cancer stem cells dictates tumorigenesis and multipotency.* Oncogene, 2017. **36**(4): p. 570-584.
93. Herold-Mende, C. and A. Mock, *Microenvironment and brain tumor stem cell maintenance: impact of the niche.* Anticancer Agents Med Chem, 2014. **14**(8): p. 1065-74.

8 Erklärung zum Eigenanteil

Die Arbeit wurde im Labor für experimentelle Strahlenbiologie der Universitätsklinik für Radioonkologie unter der Betreuung von Herrn Prof. Dr. Daniel Zips und Herrn Prof. Dr. Stephan Huber durchgeführt.

Die Konzeption der Arbeit erfolgte durch Herrn Prof. Daniel Zips, Doktorvater, und Herrn Prof. Dr. Stephan Huber, Sektionsleiter Labor für experimentelle Strahlenbiologie, Betreuer der Dissertation.

Sämtliche Versuche wurden nach Einarbeitung durch Herrn Prof. Dr. Huber von mir eigenständig durchgeführt. Die statistische Auswertung erfolgte eigenständig durch mich nach Anleitung durch Prof. Dr. Stephan Huber.

Ich versichere, das Manuskript selbständig verfasst zu haben und keine weiteren als die von mir angegebenen Quellen verwendet zu haben.

Von mir experimentell erhobene Daten zur Migration von U87MG Katushka Zellen (Vgl. 3.2.5) sind in die Publikation *„BK K+ channel blockade inhibits radiation-induced migration/brain infiltration of glioblastoma cells.“ (Edalat, Stegen, Klumpp, Haehl, Schilbach, Lukowski, Kuhnle, Bernhardt, Buschauer, Zips, Ruth, Huber; Oncotarget 2016 [55])* eingeflossen, an der ich als Koautor mitgewirkt habe. Aus dieser Publikation zitiere ich im Methodenteil dieser Arbeit. Im Ergebnisteil dieser Arbeit sind weder textuelle noch bildliche Übernahmen aus der genannten Publikation enthalten.

Tübingen, 2020

9 Veröffentlichungen

Teile der vorliegenden Dissertation wurden bereits veröffentlicht:

Authors:	Edalat L., Stegen B., Klumpp L., Haehl E., Schilbach K., LukowskiR. , Kuhnle M., Bernhardt G., Buschauer A., Zips D., Ruth P., Huber S.
Titel:	*BK K+ channel blockade inhibits radiation-induced migration/brain infiltration of glioblastoma cells*
Journal:	Oncotarget, Vol. 7, Issue 12
Year:	2016

10 Table of figures

Figure 1. Co-cultures of the human glioblastoma cells and endothelial cells. **A-D**. Direct Co-culturing of the red fluorescent U-87MG-Katushka glioblastoma cells on top of an endothelial cell monolayer. Given are a fluorescence micrograph of the glioblastoma monoculture (A), a light micrograph of an endothelial cell monolayer (B), a superimposed fluorescence/light micrograph of a glioblastoma/endothelial cell co-culture (C) as well as a dot blots (D) showing the Katushka fluorescence and the forward scatter of glioblastoma cells in monoculture (top) and in co-culture with endothelial cells (bottom) as recorded by flow cytometry. **E**. Scheme depicting the filter-separated co-culturing of endothelial cells with human U-87MG-Katushka or T98G glioblastoma cells. 18

Figure 2. Endothelial (HUVEC) and U-87MG-Katushka glioblastoma cells express SDF-1 protein. **A-C.** Fluorescence micrographs of U-87MG-Katushka cells grown in monoculture (A) or direct co-culture with endothelial cells (B-C) showing DAPI-stained nuclei (blue, outer left), Katushka protein (red, middle left), SDF-1 protein (A-B, green, middle right), or staining elicited by an unspecifically bound IgG isotype control antibody (C, green, middle right), or all three fluorochroms in overlay (outer right). **D.** Overlay of DAPI- (blue), Katushka- (red), and SDF-1 (green)-specific fluorescence micrographs of a direct U-87MG-Katushka/endothelial cell co-culture in higher power. **E.** Quantified mean (± SE, n = 62-111 cells) SDF-1-specific fluorescence intensity of U-87MG-Katushka cells in monoculture (white), U-87MG-Katushka cells in direct co-culture with endothelial cells (black), and endothelial cells in direct co-culture with U-87MG-Katushka cells (green). * indicates $p \leq 0.05$, Kruskal-Wallis test (nonparametric ANOVA) and Dunn's Multiple Comparisons post test. 34

Figure 3 Endothelial cells (HUVEC) have no protective or radiosensitizing effect on apoptotic cell death of U-87MG-Katushka cells. **A.** Dot blots plotting the Katushka fluorescence against the side scatter as recorded by flow cytometry in direct U-87MG-Katushka/endothelial cell (hCMEC/D3) co-cultures. **B.** Mean (± SE, n = 8) Annexin V fluorescence intensity of U-87MG-Katushka cells (as recorded in A) grown in monoculture (open bars) or direct U-87MG-Katushka/endothelial cell co-culture (closed

bars) with or without single-time radiation of 6 Gy. * indicates p ≤ 0.01, two-tailed (Welch corrected) t-test. 35
Figure 4. Endothelial cells (HUVEC) do not alter clogenic survival or radioresistance of T98G cells. **A** 6-well scans showing Coomassie-stained colonies formed from 300 plated control (0 Gy) or irradiated (4 Gy) cells. **B-C** mean (± SE, n = 54) plating efficacy and mean survival fractions at different radiation dose of T98G cells grown in monoculture (open bars and symbols) or in filter-separated co-cultures with endothelial cells (closed bars and red symbols). 35
Figure 5. Endothelial cells (hCMEC/D3) co-culture does not alter radiation induced cell death. **A.** Histograms depicting the CasPACE fluorescence of Katushka-positive cells as recorded by flow cytometry in U-87MG-Katushka monocultures (top) and direct U-87MG-Katushka/endothelial cell (hCMEC/D3) co-cultures (bottom). **B.** Mean (± SE, n = 6-8) CasPACE fluorescence intensity of U-87MG-Katushka cells (as recorded in A) grown in monoculture (open bars) or direct U-87MG-Katushka/endothelial cell co-culture (closed bars) with or without single-time radiation of 6 Gy. * indicates p ≤ 0.01, two-tailed (Welch corrected) t-test. 36
Figure 6. Endothelial (hCMEC/D3) co-culture does not alter clogenic survival or radioresistance of U-87MG-Katushka and T98G cells. A 6-well scans showing Coomassie-stained colonies formed from 300 plated control (0 Gy) or irradiated (4 Gy) cells. B-C mean (± SE, n = 54) plating efficacy and mean survival fractions at different radiation dose of U-87MG-Katushka cells grown in monoculture (open bars and symbols) or in filter-separated co-cultures with endothelial cells (closed bars and red symbols)..... 37
Figure 7. Directly co-cultured endothelial cells (hCMEC/D3) lower mRNA abundance of the ion channel TRPM8 in U87MG-Katushka glioblastoma cells. **A.** Houskeeper-normalized mRNA abundances of the endothelial cell marker Von-Willebrand-factor (vWF) in endothelia cell monocultures (1st bar), in U-87MG-Katushka grown in monocultures (2nd bar) and direct co-cultures with endothelial cells (3rd bar). **B-E**. Houskeeper-normalized abundances of mRNAs encoding for stem cell markers (B), ion channels (C), chemokine signaling (D), and TGF-beta signaling (E). Mean data (± SE, n =

3-4) of U-87MG Katushka cells grown in monoculture (open bars) and co-culture (closed bars) with endothelial cells are shown. Irradiated and non-irradiate samples pooled. * indicate p ≤ 0. 05, two-tailed Welch corrected *t*-test. 39
Figure 8. Transfilter co-cultured endothelial cells (hCMEC/D3) induce upregulation of mRNAs involved in cell migration and invasion in U87MG-Katushka glioblastoma cells. **F-L**. Houskeeper-normalized abundances of mRNAs encoding for stem cell markers (F+G), ion channels (H), chemokine signaling (I), endothelial von-Willebrand factor (J), TGF-beta signaling (K), and matrix metalloproteinase (I). Mean data (± SE, n = 4-10) of U-87MG-Katushka cells grown in monoculture (open bars) and filter-separated co-culture (closed bar) with endothelial cells are shown. Irradiated and non-irradiate samples pooled. * and ** indicate p ≤ 0. 05 and p ≤ 0.01, respectively, two-tailed Welch corrected t-test. 40
Figure 9. Endothelial cells (hCMEC/D3) induce activation of outward currents in U-87MG-Katushka glioblastoma cells. **A**. Schemes, depicting the pipette and bath solution (top) and the voltage pulse protocol (bottom) applied in on-cell (cell-attached) patch clamp experiments. **B**. Representative on-cell current tracings recorded with the protocol illustrated in (A) in U-87MG-Katushka cells grown in monoculture (left) or direct co-culture with endothelial cells (right). Zero current is indicated by red line, macroscopic current tracings of the individual current sweeps recorded at the different clamp-voltages are superimposed. **C**. Relationship between mean (± SE, n = 9-11 cells) macroscopic on-cell currents and voltage recorded as in (A, B) in U-87MG-Katushka cells grown in monoculture (open circles) or direct co-culture with endothelial cells (closed triangles). **D, E**. Mean (± SE) conductance (D) and reversal potential (E) of the macroscopic on-cell current in U-87MG-Katushka cells grown in monoculture (open bars) or direct co-culture with endothelial cells (closed bars). Data from (C), conductances were calculated by linear regression between +35 mV and + 60 mV (as indicated in (C) by blue and red line). ** indicates p ≤ 0.01, two-tailed (Welch corrected) t-test. 43
Figure 10. Large conductance, voltage-dependent K+-selective channels generate the outward current induced by endothelial cell (hCMEC/D3) in U-87MG-Katushka cells. **A**.

Current tracings of a U-87MG-Katushka cells directly co-cultured with endothelial cells recorded at different holding potentials (as indicated) in on-cell mode with NaCl in bath and pipette solutions. **B, E**. Relationship between mean (± SE, n = 3-6) channel amplitude (B) or open probability (nPo, E) and holding potential recorded in U-87MG-Katushka cells grown in monoculture (open circles) or direct co-culture with endothelial cells (closed triangles). **C, D, F**. Conductance (C), reversal potential (D), and open probability (F) of channels recorded in mono- (open circles) and co-cultured U-87MG-Katushka cells (closed triangles). Individual recordings are shown. Conductances in (C) and open probabilities in (F) were given for positive holding potentials (as indicated by red and blue line in (B)) and physiological membrane potential (i.e., 0 mV holding potential), respectively. n. d.: not determinable. 44

Figure 11. Endothelial cells stimulate transfilter chemotaxis of U-87MG-Katushka cells. **A**. Time course of changes in mean (± SE, n = 28-29) impedance as a real time measure of transfilter chemotaxis (1%/5% FCS gradient) as recorded with the Roche xCelligence Sytem in U87MG-Katushka cells grown in monoculture (open circles) or filter-separated co-culture with endothelial cells (closed triangles). **B**. Transfilter chemotaxis-dependent impedance increase as defined by the slope of the impedance/time relationship between 0 and 1.5 h of monocultured (open circles) and co-cultured U87MG-Katushka cells. Shown are individual experiments, data from (A). ** indicates $p \leq 0.01$, Welch-corrected t-test. 45

11 Danksagung

Ich möchte mich ganz herzlich bei folgenden Personen bedanken:

Bei Herrn Professor D. Zips für die Überlassung und Heranführung an dieses spannende Thema, die strukturelle Unterstützung durch die Klinik für Radioonkologie, sowie für Supervision und Begutachtung der Promotion.

Bei Herrn Professor Stephan Huber für die umfassende und engagierte Betreuung der Arbeit in Einarbeitung, Durchführung und Verschriftlichung, sowie den vielfältigen Austausch auch über die Strahlenbiologie hinaus.

Bei Dominik Klumpp, Lukas Klumpp und Benjamin Stegen für die methodische Einarbeitung und die produktive und heitere Laboratmosphäre.

Ich denke an Herrn D., den ersten Patienten mit Glioblastom, den ich betreut habe, und der stets darauf bestand mich Doktor zu nennen. Leider habe ich auch durch ihn erfahren, welches furchtbare Schicksal diese Krankheit bedeutet.

Bei Julia Küppers für die ausdauernde Motivation beim Fertigstellen dieser Arbeit und für deine Liebe.

Bei meiner Mutter Sibylle Haehl, die während der schweren Zeit nach dem Tod unseres Vaters für uns drei Geschwister so viel geleistet und auf so vieles verzichtet hat, darunter ihre eigene Promotion. Ihr ist diese Arbeit gewidmet.

12 Appendix

Table 7: Cell lines

Cell line	Type	Origin	Medium
T98G	human glioblastoma	ATCC	RPMI 1640 +10% FBS
U87MG „Katushka“	human glioblastoma, fluorescent protein transfected [55]	ATCC	RPMI 1640 +10% FBS +G418 (750µg/ml)
HUVEC	human umbilical vein endothelial cells	Department of neurosurgery UKT	VascuLife EnGS Kit
HCMEC/D3	human cerebral microvascular endothelial cells	Merck-Millipore (Cat. No. SCC066)	EndoGRO-MV Complete Cluture Media kit

Table 8: Media

Medium	Cell line	Catalogue number	Distributor
VascuLife EnGS Kit	HUVEC	LL-0002	Lifeline cell technology, Frederick, USA
EndoGRO-MV Kit	hCMEC/D3	SCME004	Merck-Millipore, Darmstadt, Germany
Dulbecco’s Modified Eagle’s	T98G	D5546	Sigma Aldrich, St. Louis, USA
RPMI 1640	U-87MG Katushka	R0883	Sigma Aldrich, St. Louis, USA
Fetal calf serum	all	S0615	Biochrom GmbH, Berlin, Germany

Table 9. Cell culture substances

Substance	**Description**	**Catalogue number**	**Distributor**
Gelatin	Gelatin from bovine skin	G9391	Sigma-Aldrich, St. Louis, USA
Trypsin	protease	25300054	Thermo Fisher Scientific, Waltham, USA
CDS	Enzyme Free Cell Dissociation Solution	S-014B	Millipore, Darmstadt, Germany
DMSO	Cryoprotectant	D2650	Sigma-Aldrich, St. Louis, USA
Collagen	Collagen R solution 0,2%	47254.02	Serva Electrophoresis, Heidelberg, Germany
b-FGF	Recombinant Human FGF basic	233-FB	R&D Systems, Minneapolis, USA

Table 10: Cell culture tools

Tool	**Description**	**Catalogue number**	**Distributor**
Trans-filter insert	ThinCert, 6-well, 3µm	657630	Greiner Bio-one, Frickenhausen, Germany
Cell freezing container	Nalgene® Cryo 1°C “Mr. Frosty”	5100-0001	Nalge Nunc Internaional, Penfield, USA
Millicell EZ object slides	8-Well	PEZGS0816	Millipore, Darmstadt, Germany

Table 11: Devices

Device	Name	Manufacturer
CIM-Plate 16		Roche, Mannheim, Germany
Inkubator	HeraCell 240	Heraeus, Hanau, Germany
PCR platform	LightCycler 480	Roche, Mannheim, Germany
Thermalcycler	Mastercycler personal	Eppendorf, Hamburg, Germany
Spectrophotometer	Nano Drop 1000	Nano Drop Technologies, Wilmington, USA
Linear accelerator	LINAC SL25	Philips/Elekta, Stockholm, Sweden
Laminar flow system	BDK-SBV	Weiss Technik, Altendorf, Switzerland
xCELLigence	RTCA DP	ACEA Bioscience, San Diego, USA
Centrifuge	Centrifuge 5804R	Eppendorf, Hamburg, Germany

Table 12: Agents for colony formation assay, migration assay, flow cytometry and immunofluorescence

Substance	Description	Catalogue number	Distributor
Brillant Blue R-250	biological cell stain for ptoteins	B0149-25G	Sigma-Aldrich, St. Louis, USA
Annexin-V-Fluos	Fluorescence-conjugated anticoagulant	11828681001	Roche Life Science, Mannheim, Germany
CaspACE	CaspACE FITC VAD-FMK	G7462	Promega, Madison, USA
SDF-1 Antibody	Polyclonal, Rabbit	NBP1-19778	Novus Biologicals, Bio-Techne, Minneapolis, USA

IgG Isotype control	Normal rabbit IgG	12-370	Merck-Millipore, Darmstadt, Germany
	Goat anti-Rabbit IgG Antibody	NB730-F	Novus Biologicals, Bio-Techne, Minneapolis, USA
Triton X-100	Detergent	3051.4	Carl Roth, Karlsruhe, Germany
BSA	Bovine serum albumine	8076.4	Carl Roth, Karlsruhe, Germany